

## Article

# Emerging Role of Oxidative Stress on EGFR and OGG1-BER Cross-Regulation: Implications in Thyroid Physiopathology

Carmelo Moscatello<sup>1</sup>, Maria Carmela Di Marcantonio<sup>2</sup> , Luca Savino<sup>2</sup> , Emira D'Amico<sup>1</sup>, Giordano Spacco<sup>1</sup>, Pasquale Simeone<sup>3,4</sup> , Paola Lanuti<sup>3,4</sup>, Raffaella Muraro<sup>2</sup>, Gabriella Mincione<sup>2</sup>, Roberto Cotellese<sup>1,5</sup> and Gitana Maria Aceto<sup>1,\*</sup> 

- <sup>1</sup> Department of Medical, Oral and Biotechnological Sciences, University "G. d'Annunzio" Chieti-Pescara, Via dei Vestini 31, 66100 Chieti, Italy; carmelo.moscatello@unich.it (C.M.); emira.damico@unich.it (E.D.); giordano.spacco@studenti.unich.it (G.S.); roberto.cotellese@unich.it (R.C.)
- <sup>2</sup> Department of Innovative Technologies in Medicine & Dentistry, University "G. d'Annunzio", Chieti-Pescara, Via dei Vestini 31, 66100 Chieti, Italy; dimarcantonio@unich.it (M.C.D.M.); luca.sav@hotmail.it (L.S.); raffaella.muraro@unich.it (R.M.); gabriella.mincione@unich.it (G.M.)
- <sup>3</sup> Department of Medicine and Aging Sciences, University "G. d'Annunzio", Chieti-Pescara, 66100 Chieti, Italy; pasquale.simeone@unich.it (P.S.); paola.lanuti@unich.it (P.L.)
- <sup>4</sup> Center for Advanced Studies and Technology (C.A.S.T.) at University "G. d'Annunzio", Chieti-Pescara, 66100 Chieti, Italy
- <sup>5</sup> Villa Serena Foundation for Research, 66013 Pescara, Italy
- \* Correspondence: gitana.aceto@unich.it; Tel.: +39-0871-355-4115



**Citation:** Moscatello, C.; Di Marcantonio, M.C.; Savino, L.; D'Amico, E.; Spacco, G.; Simeone, P.; Lanuti, P.; Muraro, R.; Mincione, G.; Cotellese, R.; et al. Emerging Role of Oxidative Stress on EGFR and OGG1-BER Cross-Regulation: Implications in Thyroid Physiopathology. *Cells* **2022**, *11*, 822. <https://doi.org/10.3390/cells11050822>

**Academic Editors:**  
Evangelos Kolettas and  
Vassilis Gorgoulis

Received: 30 November 2021

Accepted: 23 February 2022

Published: 26 February 2022

**Publisher's Note:** MDPI stays neutral with regard to jurisdictional claims in published maps and institutional affiliations.



**Copyright:** © 2022 by the authors. Licensee MDPI, Basel, Switzerland. This article is an open access article distributed under the terms and conditions of the Creative Commons Attribution (CC BY) license (<https://creativecommons.org/licenses/by/4.0/>).

**Abstract:** Thyroid diseases have a complex and multifactorial aetiology. Despite the numerous studies on the signals referable to the malignant transition, the molecular mechanisms concerning the role of oxidative stress remain elusive. Based on its strong oxidative power, H<sub>2</sub>O<sub>2</sub> could be responsible for the high level of oxidative DNA damage observed in cancerous thyroid tissue and hyperactivation of mitogen-activated protein kinase (MAPK) and PI3K/Akt, which mediate ErbB signaling. Increased levels of 8-oxoG DNA adducts have been detected in the early stages of thyroid cancer. These DNA lesions are efficiently recognized and removed by the base excision repair (BER) pathway initiated by 8-oxoG glycosylase1 (OGG1). This study investigated the relationships between the EGFR and OGG1-BER pathways and their mutual regulation following oxidative stress stimulus by H<sub>2</sub>O<sub>2</sub> in human thyrocytes. We clarified the modulation of ErbB receptors and their downstream pathways (PI3K/Akt and MAPK/ERK) under oxidative stress (from H<sub>2</sub>O<sub>2</sub>) at the level of gene and protein expression, according to the mechanism defined in a human non-pathological cell system, Nthy-ori 3-1. Later, on the basis of the results obtained by gene expression cluster analysis in normal cells, we assessed the dysregulation of the relationships in a model of papillary thyroid cancer with RET/PTC rearrangement (TPC-1). Our observations demonstrated that a H<sub>2</sub>O<sub>2</sub> stress may induce a physiological cross-regulation between ErbB and OGG1-BER pathways in normal thyroid cells (while this is dysregulated in the TPC-1 cells). Gene expression data also delineated that *MUTYH* gene could play a physiological role in crosstalk between ErbB and BER pathways and this function is instead lost in cancer cells. Overall, our data on OGG1 protein expression suggest that it was physiologically regulated in response to oxidative modulation of ErbB, and that these might be dysregulated in the signaling pathway involving AKT in the progression of thyroid malignancies with RET/PTC rearrangements.

**Keywords:** oxidative stress; ErbB receptors; OGG1; *MUTYH*; BER; RET/PTC; PI3K/Akt; MAPK/ERK; thyroid; PTC

## 1. Introduction

Over the last 30 years, the incidence rate of thyroid cancer has steadily increased by 2.4 times [1,2] and papillary thyroid carcinoma (PTC) represents the most common histological type, with a frequency around 80% of cases [1]. Carcinogenesis and tumor progression

in the thyroid gland are a phenotypic expression of a complex molecular interaction based on the connection between gene predisposition, environmental factors, and lifestyle, the effects of which influence thyroid hormone metabolism and oxidative DNA damage [3,4]. Oxidative damage has been suggested to promote tumor initiation and progression by increasing mutation rates and activating oncogenic pathways. Thyroid hormone synthesis is a complex and multistep physiological process that requires an adequate amount of  $H_2O_2$  for oxidative iodination catalyzed by the enzyme thyroid peroxidase (TPO) [5–8]. On the other hand, based on its strong oxidative power,  $H_2O_2$ , could be responsible for the high level of oxidative DNA damage as observed in thyroid cancer tissue; it is also considered a second messenger able to activate several signaling pathways [9,10]. Oxidative DNA lesions have been detected in advanced stages of thyroid cancer, suggesting their contribution to tumor progression [4]. In recent years, there has been a growing interest in studying the role of oxidative stress in cancer initiation/progression and therapeutic response [11]. Indeed,  $H_2O_2$  is also a signaling molecule involved in both the regulation of cell proliferation and apoptosis [10].

In cancer cells,  $H_2O_2$  may regulate EGFR and mitogen-activated protein kinase (MAPK) signaling that contribute to redox protein-mediated cancer progression [12]. In addition, high levels of ROS have been found in thyroid adenomas and early stages of cellular transformation along with decreased antioxidant enzymes. Indeed, both oxidative stress and DNA damage are thought to be events that precede neoplasia in thyroid cells. [13] Such a circumstance, present in chronic thyroiditis, may contribute to the development of papillary thyroid carcinoma (PTC) [14].  $H_2O_2$  has been shown to cause the RET/PTC1 rearrangement frequently found in radiation-induced PTCs [15]. A marked increase in the presence of 8-oxoG in nuclear and mitochondrial DNA was evident after treatment with  $H_2O_2$  or ionizing radiation [16]. Of the various types of oxidative DNA damage, 8-oxo-7,8-dihydroguanine (8-oxoG), has been reported as the most abundant. Despite its mild cytotoxicity, the 8-oxoG incorporation into DNA may be mutagenic since it causes a high transversion mutation rate [17–19]. Increased levels of the 8-oxoG DNA adducts have been detected in early stages of thyroid cancer: this may contribute to mutagenesis resulting in increased cell proliferation and survival [20]. The 8-oxoG DNA lesion is recognized and efficiently removed by 8-oxoG glycosylase1 (OGG1)-initiated base excision repair (BER) pathway (OGG1-BER) [20–22]. OGG1 glycosylase protects DNA from mutagenic potential caused by 8-oxoG:A mismatch leading to G:C to T:A transversion. Therefore, a correct function of OGG1-BER can be considered a protective factor against the triggering of carcinogenic pathways [20,21].

The involvement of EGFR signaling in thyroid carcinogenesis has been documented for a long time [23,24] and a link between DNA repair mechanisms and epidermal growth factor receptor (EGFR) signaling has been reported in many human tumor cells [25–27]; however, their cross-regulation is poorly understood in thyroid pathophysiology.

All these observations prompted us to study the existence of cross-regulation between EGFR- and OGG1-BER-related molecular pathways in thyrocytes under  $H_2O_2$ -mediated acute oxidative stress.

For our purpose, we compared a thyroid cancer (PTC) model with a normal cell counterpart to better identify changes in molecular signaling under specific treatment conditions, that would alter biological pathways for maintaining normal cell function. We chose to use a system of immortalized normal cells, Nty-ori 3-1, and a human model of differentiated papillary thyroid cancer (TPC-1 cells). In the context of papillary carcinoma cell lines, the TPC-1 line has no mutations other than RET/TPC rearrangement [28].

This allowed us to elucidate how modulation of ErbB receptors and their downstream pathways (PI3K/Akt and MAPK/ERK) under acute oxidative stress are able to influence the molecular relationships with the OGG1-BER pathway.

## 2. Materials and Methods

### 2.1. Cell Culture and Treatments

Human thyroid follicular epithelial Nthy-ori 3-1 cells, obtained from European Collection of Authenticated Cell Cultures (ECACC 90011609) (Public Health England, Porton Down, Salisbury, UK) (Sigma Aldrich, St. Louis, MO, USA) were cultured at 37 °C in RPMI 1640 medium containing 10% fetal bovine serum (FBS), 100 U/mL penicillin/streptomycin and 2 mM L-glutamine. Human thyroid cancer cell lines, TPC-1 (harboring RET-PTC rearrangement, BRAF WT/WT), characterized according to Schweppe et al., and kindly provided by A. Coppa (Department of Experimental Medicine, Sapienza University of Rome, Rome), were maintained in a 5% CO<sub>2</sub> culture humidified atmosphere, at 37 °C in Dulbecco's modified Eagle medium (DMEM) supplemented with 10% FBS [29]. For experiments, cells were seeded and at sub-confluence (70%), were starved overnight using medium with 0.2% FBS, in order to reduce basal cellular activity [30,31]. Then, the cells were stressed by H<sub>2</sub>O<sub>2</sub> (Sigma-Aldrich, Milan, Italy) alone or combined with EGF (human recombinant, Sigma Aldrich) or MAPK and AKT inhibitors (PD98059 and LY294002, respectively). In particular, the cells were pretreated with 50 ng/mL EGF for 15 min or with PD98059 (PD) at 50 µM and LY294002 (LY) at 25 µM (Cell Signaling Technology, Beverly, MA, USA) for 1 h and then stressed by a supra-physiological H<sub>2</sub>O<sub>2</sub> concentration added to the external medium.

### 2.2. Cell Viability Assay

To assess the H<sub>2</sub>O<sub>2</sub> effects on cell viability, Nthy-ori 3-1 and TPC-1 cells were cultured in 96-well plate (1.0 × 10<sup>4</sup> cells/well) for 48 h, starved overnight using medium with 0.2% FBS and then exposed to supra-physiological H<sub>2</sub>O<sub>2</sub> increasing concentration (from 50 µM to 10 mM) at different times (3, 6 and 24 h). This was followed by incubation with 10 µL/well of 2-[2-methoxy-4-nitrophenyl]-3-[4-nitrophenyl]-5-[2,4-disulphophenyl]-2H-tetrazolium, monosodium salt (MTS) assay (Promega, Madison WI, USA) at 37 °C for 1 h. Cell viability was evaluated at 490 nm using the GloMax-Multi Detection System (Promega). The MTS assay is an indirect measure of cell number/vitality based on mitochondrial metabolic activity. The H<sub>2</sub>O<sub>2</sub> stressor concentration range was chosen based on the physiological amounts of H<sub>2</sub>O<sub>2</sub> reported as being produced *in vitro* by proliferating thyroid models [31].

### 2.3. Flow Cytometry and Cell Cycle Assay

The effect of limit H<sub>2</sub>O<sub>2</sub> stress on the quality of cell cycle at short time points was evaluated by flow cytometry cell cycle analyses (FACS) on normal and tumor cell lines. The cells were seeded on 6 cm plate at a density of 0.8 × 10<sup>6</sup>; at sub-confluence (70%), the cells were starved overnight (with 0.2% FBS), then were treated with H<sub>2</sub>O<sub>2</sub> 10 mM for a short time (15 and 30 min). FACS analysis were carried out as already reported [32,33]. Briefly 3 × 10<sup>5</sup> cells/sample were fixed by adding 500 µL of 70 % cold ethanol and then stored at 4 °C. After at least 24 h, samples were washed and stained by 500 µL of a solution composed of 50 µg/mL of propidium iodide (PI, Sigma) and 200 µg/mL of RNase (Sigma). Cells were incubated overnight at 4 °C in the dark and then acquired by flow cytometry. PI fluorescence data were collected using linear amplification. Samples were acquired on a FACSCanto II flow cytometer (Becton Dickinson Biosciences, San Jose, CA, USA). Data were analyzed using the FlowJo software (Becton Dickinson Biosciences).

### 2.4. Real-Time Quantitative PCR Analysis (qRT-PCR)

For gene expression experiments, the cells were seeded on 10 cm plate at a density of 3.2 × 10<sup>4</sup>; at sub-confluence (70%), starved overnight using medium with 0.2% FBS, then the cells were treated with H<sub>2</sub>O<sub>2</sub> alone or combined EGF or MAPK and AKT inhibitors (PD98059 and LY294002, respectively) and then acutely stressed for 15 and 30 min with a concentration of H<sub>2</sub>O<sub>2</sub> (10 mM) determined on the basis of MTS and FACS assays.

Total RNA was isolated using TriFast (EUROGOLD EuroClone) according to the manufacturer's instructions. The synthesis of complementary DNA (cDNA) was performed

as previously described [34]. The mRNA levels were evaluated by SYBR Green quantitative real-time PCR (qRT-PCR) analysis using StepOne™ 2.0 (Applied Biosystems, Thermo Fisher Scientific, Waltham, MA, USA). Data were analyzed using the comparative Ct method and were graphically indicated as  $2^{-\Delta\Delta C_t} + SD$ . In accordance with the method, the mRNA amounts of the target genes were normalized by the ratio on the median value of the endogenous housekeeping gene (*GUSB*) obtained in each treated cells vs. untreated (quiescent) cells.

Targets and reference genes were amplified in triplicate in a volume of 10  $\mu$ L containing 1  $\mu$ L template cDNA, 0.2  $\mu$ L of primers mixture and 5  $\mu$ L of GoTaq® 2-Step RT-qPCR System (Promega) according to the manufacturer's instructions. Primers sequences are available in Table S1. The cycling conditions were performed as follows: 10 min at 95 °C and 40 cycles of 15 s at 95 °C, followed by 1 min at 60 °C, and final elongation of 15 s at 95 °C.

### 2.5. Gene Dosage Assay of *OGG1* and *MUTYH*

Two different genomic target sequences were selected for *OGG1* (GeneID: 4968; Gene Bank accession number: NM\_016821) and *MUTYH* (GeneID: 4595; Gene Bank accession number: NM\_12222.1). Genomic DNA was extracted as previously described [35] and gene dosage was performed by SYBR Green qRT-PCR. The samples were amplified in triplicate in three independent experiments. Data were analyzed using  $2^{-\Delta\Delta C_t} + SD$ . In accordance with the qRT-PCR method, previously described, the gDNA amounts of the target genes were normalized by the ratio on median value of the  $\beta$ -Actin as genomic reference from TPC-1 vs. Nthy-ori 3-1. Primers sequences are listed in Table S1.

### 2.6. Western Blotting

For protein expression experiments, Nthy-ori 3-1 and TPC-1 cells were seeded on 10 cm plate at  $3.2 \times 10^4$  density, at sub-confluence the cells were starved overnight and then acutely stressed by 10 mM H<sub>2</sub>O<sub>2</sub> for 15 and 30 min alone or combined with EGF or PD or LY. Total proteins were isolated from treated and untreated cells using lysis buffer [2 mM Na<sub>3</sub>VO<sub>4</sub>, 4 mM sodium pyrophosphate, 10 mM sodium fluoride, 50 mM HEPES pH 7.9, 100 mM NaCl, 10 mM EDTA, 1% Triton X-100, 2  $\mu$ g/mL leupeptin, 2  $\mu$ g/mL aprotinin, 1 mM PMSF]. Protein concentrations were determined using the BCA protein assay (Thermo Fisher Scientific, Waltham, CA, USA). An equal amount of total proteins was separated on 4–20% SDS-PAGE pre-cast gel electrophoresis (Bio-Rad Laboratories, Hercules, CA, USA) and transferred onto PVDF membranes (GE Healthcare, Chicago, IL, USA). Then, after blocking, the membranes were incubated with primary antibody overnight at 4 °C. The following primary antibodies were used: phospho-p44/42 MAPK, phospho-AKT, phospho-EGFR (Tyr1068), PARP-1 (Cell Signaling Technology); EGFR (Santa Cruz Biotechnology, Santa Cruz, CA, USA); ErbB2 (Dako, Santa Clara, CA, USA); OGG1 (Novus Biologicals, Littleton, CO, USA);  $\beta$ -actin (Sigma-Aldrich, St. Louis, MI, USA)—used as a protein loading control. Secondary antibodies were HRP-conjugated anti-rabbit or anti-mouse (Bethyl Laboratories, Montgomery, TX, USA). The immune complexes were visualized using the ECL Western blot detection system (EuroClone). Protein amounts were quantified by the Image Lab™ Software Version 5.0 (Bio-Rad Laboratories).

### 2.7. Statistical Analysis and Tools

All measurements were made after three independent experiments, and, for each, data is shown as a representative value of all experiments plus standard deviation. The results were subjected to t-test or one-way analysis of variance (ANOVA) as appropriate. All *p* values are two-sided and a *p* value of less than 0.05 was considered significant. All analyses were performed using SPSS software version 20 (IBM Corp., Armonk, NY, USA). The program Multiexperiment viewer v4.9.0 (MeV v4.9.0, J. Craig Venter Institute, La Jolla, CA, USA) [36] was employed to elucidate molecular relationship among genes expression detected in the normal Nthy-ori 3-1 cells in response to the treatments.

### 3. Results

#### 3.1. Cell Line Viability after Hydrogen Peroxide (H<sub>2</sub>O<sub>2</sub>) Treatment

In starved cells after H<sub>2</sub>O<sub>2</sub> treatment, we observed a rapid decline in cell viability, probably due to the interference of H<sub>2</sub>O<sub>2</sub> with mitochondrial activity ( $p < 0.001$ ) (Figure 1). In normal cells (Nthy-ori 3-1), viability settled at a constant value (approximately 50%) for all concentrations and times (Figure 1a). In contrast, tumor cells (TPC-1), after treatment, showed variability in their viability, at the different H<sub>2</sub>O<sub>2</sub> concentrations used (Figure 1b).

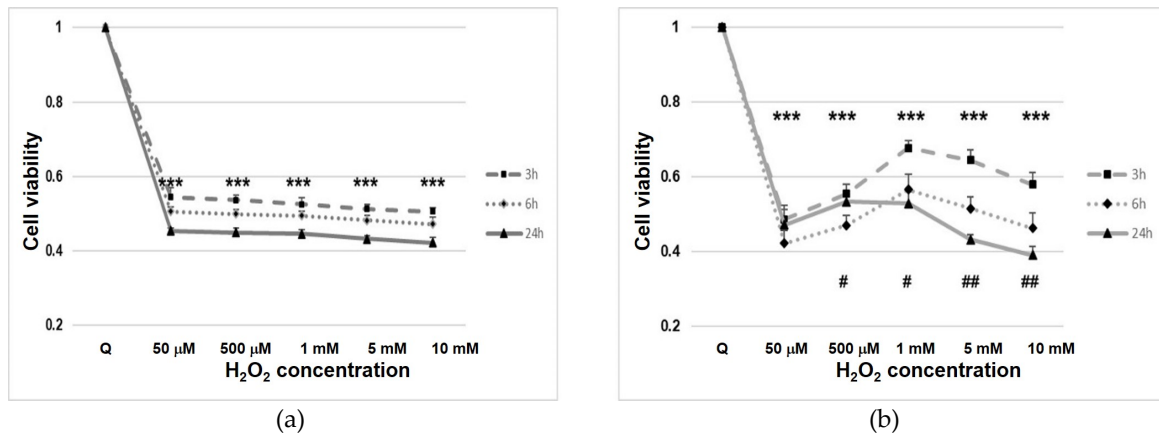


**Figure 1.** Nthy-ori 3-1 (a) and TPC-1 (b) cell line viability under H<sub>2</sub>O<sub>2</sub> stress condition. Cell viability was assayed using MTS. The cells were exposed to H<sub>2</sub>O<sub>2</sub> for different time and concentrations (from 50 μM to 10 mM). For each experiment, n = 5 replicates wells were assayed per clone. Cell viability values were calculated as means and compared with untreated quiescent cells (Q). \*\*\*— $p < 0.001$  vs. quiescent; #— $p < 0.05$ ; ##— $p < 0.01$  cells with same dosage of H<sub>2</sub>O<sub>2</sub> treatment at different time.

#### 3.2. Cell Cycle Analysis

Based on the MTS results, we evaluated the acute oxidizing effect on the cell cycle quality of treatments with the highest concentration of 10 mM to test the acute effects of H<sub>2</sub>O<sub>2</sub> at 15 and 30 min, in Nthy-ori-3-1 and TPC-1 cells. The percentages of cells in G<sub>0</sub>/G<sub>1</sub>, S and G<sub>2</sub>/M phases of the cell cycle were calculated using FlowJo software. FACS analysis on untreated Nthy-ori-3-1 underlined that 50.3 ± 6.1 % of cells were in G<sub>0</sub>/G<sub>1</sub> phase, 24.8 ± 7.9 % in S phase and 25 ± 3.0 % in G<sub>2</sub> phase in control group. The comparison with treated cells at 15 and 30 min resulted in a slight increase in the percentage of G<sub>0</sub>/G<sub>1</sub>-phase cells and in a reduction in G<sub>2</sub> phase. H<sub>2</sub>O<sub>2</sub> treatment seemed do not affect the S-phase cell population. Untreated TPC-1 cells compared with normal cells showed a higher percentage of G<sub>0</sub>/G<sub>1</sub> phase cells (73.3% ± 3.5), a lower percentage of S phase cells (9.5% ± 3.9) and the remaining 17.2 ± 5.2 in G<sub>2</sub>. Treated TPC-1 cells showed a reduction in G<sub>0</sub>/G<sub>1</sub> and an increase in G<sub>2</sub> phase cell percentage (Figure 2a,b).

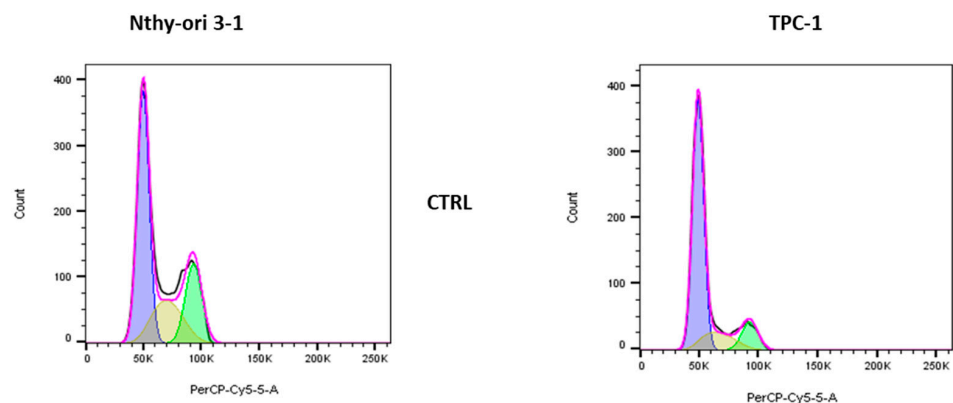


**Figure 2.** Cont.

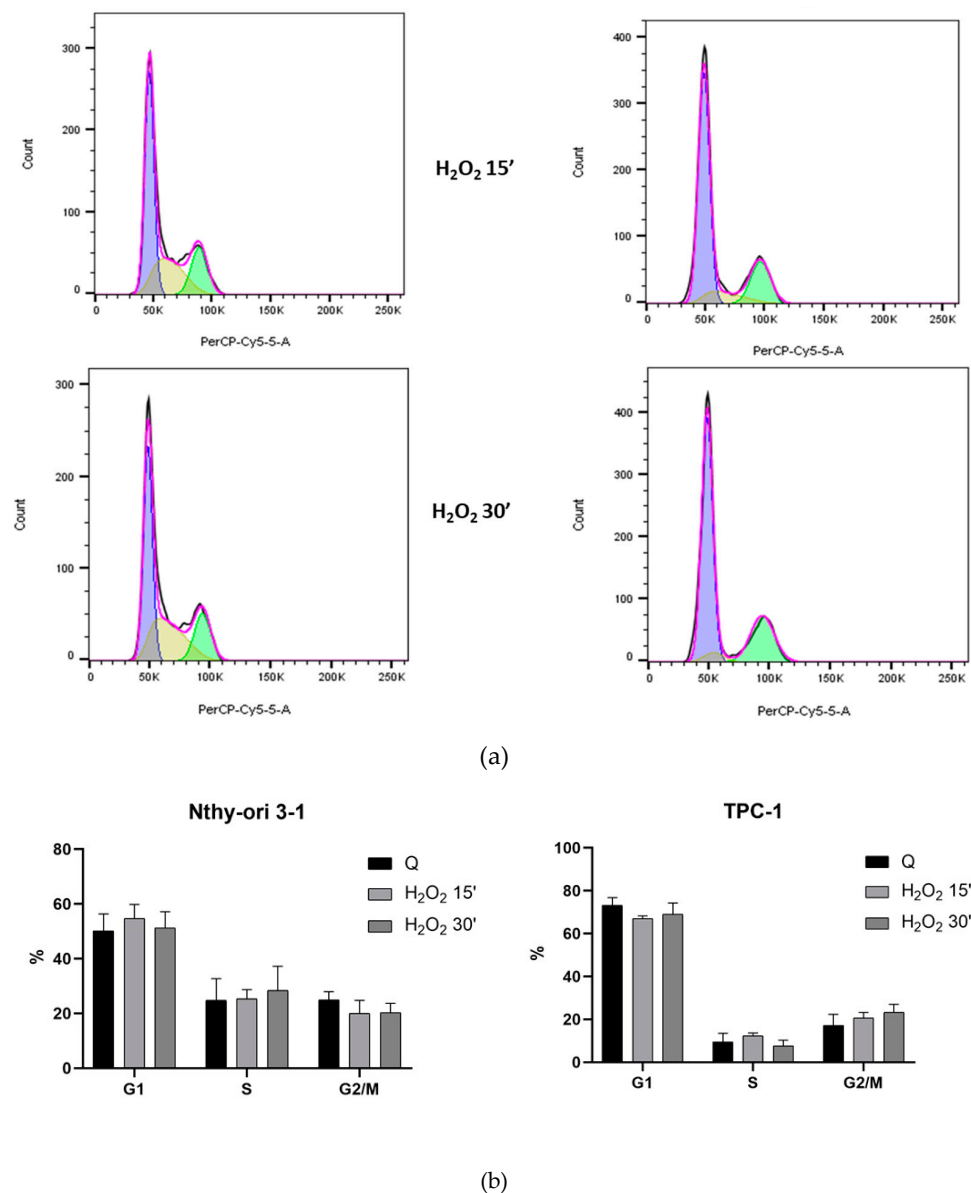


**Figure 2.** Effect of H<sub>2</sub>O<sub>2</sub> [10 mM] on the cell cycle of starved thyroid cell lines. (a) FACS analysis profile of Nthy-ori 3-1 and TPC-1 untreated and treated cells by 10 mM H<sub>2</sub>O<sub>2</sub> after 15 or 30 min; (b) relative percentages in cell cycle stages.

### 3.3. Gene Expression of BER and EGF Signaling in Nthy-ori 3-1 vs. TPC-1

Gene expression modulation of BER and EGF signaling was assayed in starved human thyroid follicular epithelial Nthy-ori 3-1 cells and starved papillary carcinoma cell line TPC-1 after short term treatments (15 and 30 min), with H<sub>2</sub>O<sub>2</sub> [10 mM], EGF, PD, LY alone or combined.

#### 3.3.1. OGG1-BER Signaling

The BER genes—*OGG1*, *MUTYH*, *APE-1/Ref-1* and *PPARγ*—in Nthy-ori 3-1 exhibited generally the same trend in the different experimental conditions (Figure 3a). These genes showed a significant ( $p < 0.05$ ) time-dependent increase, after H<sub>2</sub>O<sub>2</sub> exposure, and a significant ( $p < 0.05$ ) decrease after EGF stimulation and AKT and MAPK inhibition (Figure 3a). EGF and H<sub>2</sub>O<sub>2</sub> co-treatment increased *OGG1*, *MUTYH* and *PPARγ* compared with EGF stimulation alone; this was not observed for *APE-1*. With respect to normal cells, the TPC-1 tumor cells showed an overall gene expression deregulation, in response to the treatments (Figure 3b vs. Figure 3a). Indeed, an increase in expression after AKT inhibition

was observed for *OGG1* and *APE1*, while *PPAR $\gamma$*  and *APE1* showed an overexpression after stimulation by EGF (Figure 2b). *MUTYH* expression was not appreciably detected in TPC-1 cells (data not shown).

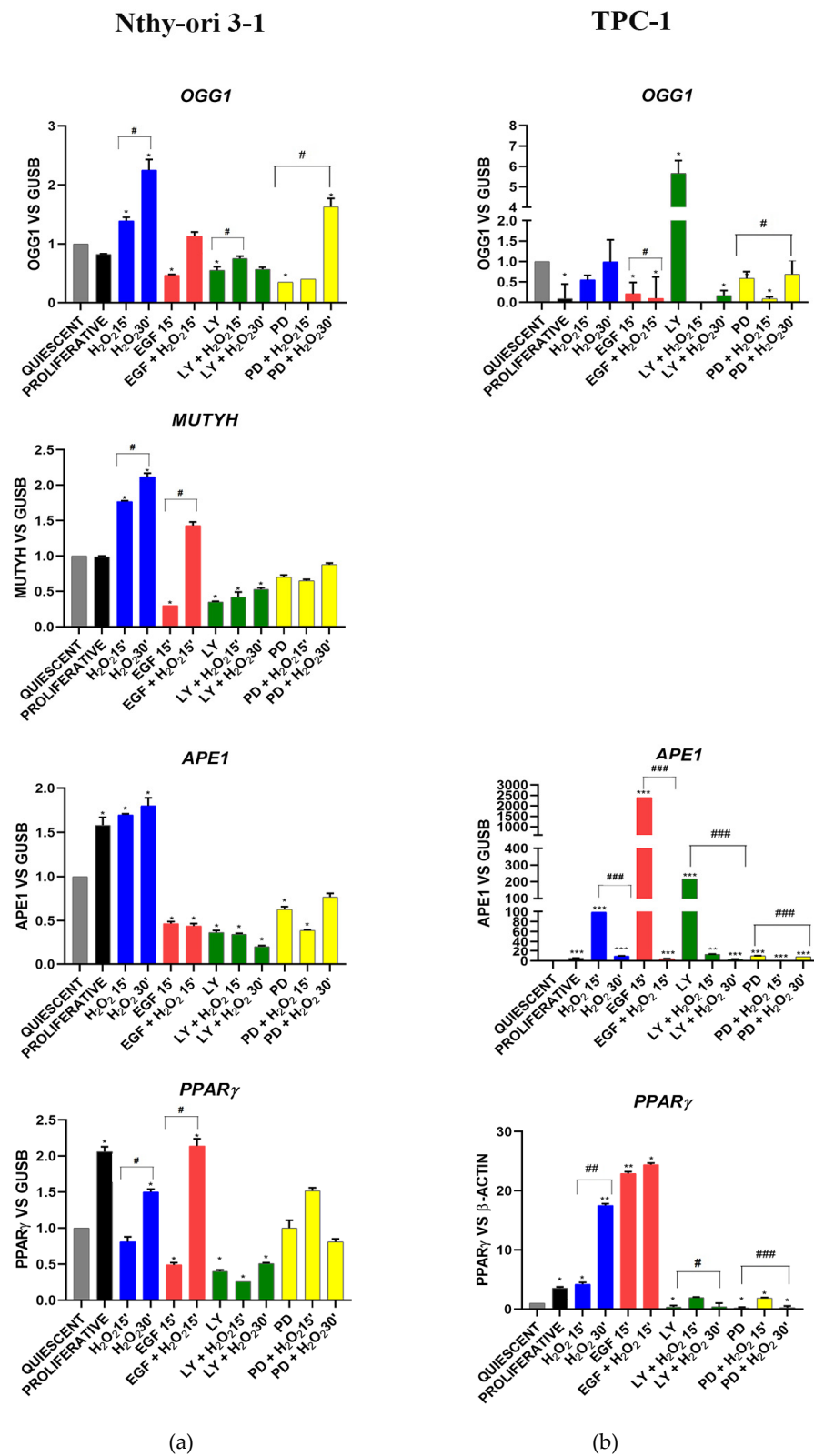


**Figure 3.** *OGG1* (8-Oxoguanine glycosylase), *MUTYH* (mutY DNA glycosylase), *APE1* (apurinic/apyrimidinic endodeoxyribonuclease-1) and *PPAR $\gamma$*  (peroxisome-proliferator-activated receptor gamma)

gene expression modulation under H<sub>2</sub>O<sub>2</sub> [10 mM], EGF, LY and PD treatments alone and combined in Nthy-ori 3-1 cells (a) vs. TPC-1 cells (b). Gene expression was analyzed by real-time qPCR. The histogram represented normalized data with *GUSB* gene in Nthy-ori 3-1, while the *PPAR*γ expression data were normalized with β-Actin in TPC-1 cells. The expression of *MUTYH* was undetected in TPC-1 cells (five independent experiments). The results showed the average of three independent experiments. LY—LY294002; PD—PD98059; \*—*p* < 0.05; \*\*—*p* < 0.01; \*\*\*—*p* < 0.001 treated vs. quiescent cells; #—*p* < 0.05; ##—*p* < 0.01; ###—*p* < 0.001 cells with similar treatment.

### 3.3.2. EGF Signaling

In Nthy-ori 3-1 cells, the stimulation with EGF and H<sub>2</sub>O<sub>2</sub>, alone or combined, did not induce any *EGFR* modulation; while LY and PD determined its overexpression and furthermore H<sub>2</sub>O<sub>2</sub> strengthened the action of inhibitors (Figure 4a). *ErbB2* expression was increased by H<sub>2</sub>O<sub>2</sub> combined with EGF and MAPK inhibitor. *ErbB2* expression was increased by co-treatment with H<sub>2</sub>O<sub>2</sub> and EGF, while it was downregulated by EGF alone and by AKT inhibitor. (Figure 4a). *ErbB3* was stimulated by EGF and PD treatments, also combined with H<sub>2</sub>O<sub>2</sub> (Figure 4a). In all conditions *ErbB4* was not detected, except after EGF stimulation (data not shown). An aberrant modulation of the *EGFR*, *ERBB2* and *ERBB3* genes was observed in TPC-1 cells. In fact, these genes tended to be repressed or poorly expressed (even in proliferating cells) but they resulted stimulated by MAPK inhibition combined with H<sub>2</sub>O<sub>2</sub> (Figure 4b).

### 3.3.3. Oxidative Stress Signaling

The gene expression levels of the molecules known to be involved in the oxidative stress response are shown in Figure 4.

In Nthy-ori 3-1, the nuclear factor erythroid-derived 2-like 2, (*NRF2*), decreased with EGF, LY and PD (alone and combined with H<sub>2</sub>O<sub>2</sub>) (Figure 5a). The inhibition by PD and PD + H<sub>2</sub>O<sub>2</sub> after 30 min increased the expression of protective antioxidant gene *HO1*, that conversely was decreased by EGF and LY inhibitor (Figure 5a). In cancer cells, *NRF2* showed a significant alteration in its expression, especially after treatment with H<sub>2</sub>O<sub>2</sub>, but also with LY and PD (Figure 5b).

In normal cells, the transcription factor *JUN/AP1* did not show any modulation following H<sub>2</sub>O<sub>2</sub>, LY and PD treatments, but its expression was increased by EGF (Figure 5a). In tumor cells, EGF stimulation resulted in overexpression of *JUN/AP1* while inhibition of AKT downregulated it (Figure 5b). The pro-inflammatory CXC chemokine *IL-8* gene (*CXCL8*) was significantly increased in normal proliferating cells compared with normal starved cells and in particular after H<sub>2</sub>O<sub>2</sub> treatments, whereas its expression was reduced by EGF stimulation and its downstream pathways (AKT and MAPK) inhibition (Figure 5a). In cancer cells, *IL-8* expression is dramatically reduced by MAPK inhibition.

### 3.3.4. Stemness and Differentiation Markers

As expected, in Nthy-ori 3-1, the expression of stem cell regulator *ZEB1* increased in proliferating cells, after EGF stimulation and in stress conditions, while its expression was decreased by LY and H<sub>2</sub>O<sub>2</sub> co-treatment (Figure 6a). Thyroid differentiation marker *TPO* showed an opposite trend in gene expression compared with *ZEB1*, except for the treatment with H<sub>2</sub>O<sub>2</sub> (Figure 6a). The reduction in *TPO* gene expression was detected following the inhibition of the AKT pathway while an opposite effect was obtained after MAPK inhibition (Figure 6a). In TPC-1 the expression of zinc finger *ZEB1* increased after LY and PD treatments, while H<sub>2</sub>O<sub>2</sub> reduced its expression (Figure 6b). In all experimental conditions, thyroid differentiation marker *TPO* resulted undetected (data not shown).

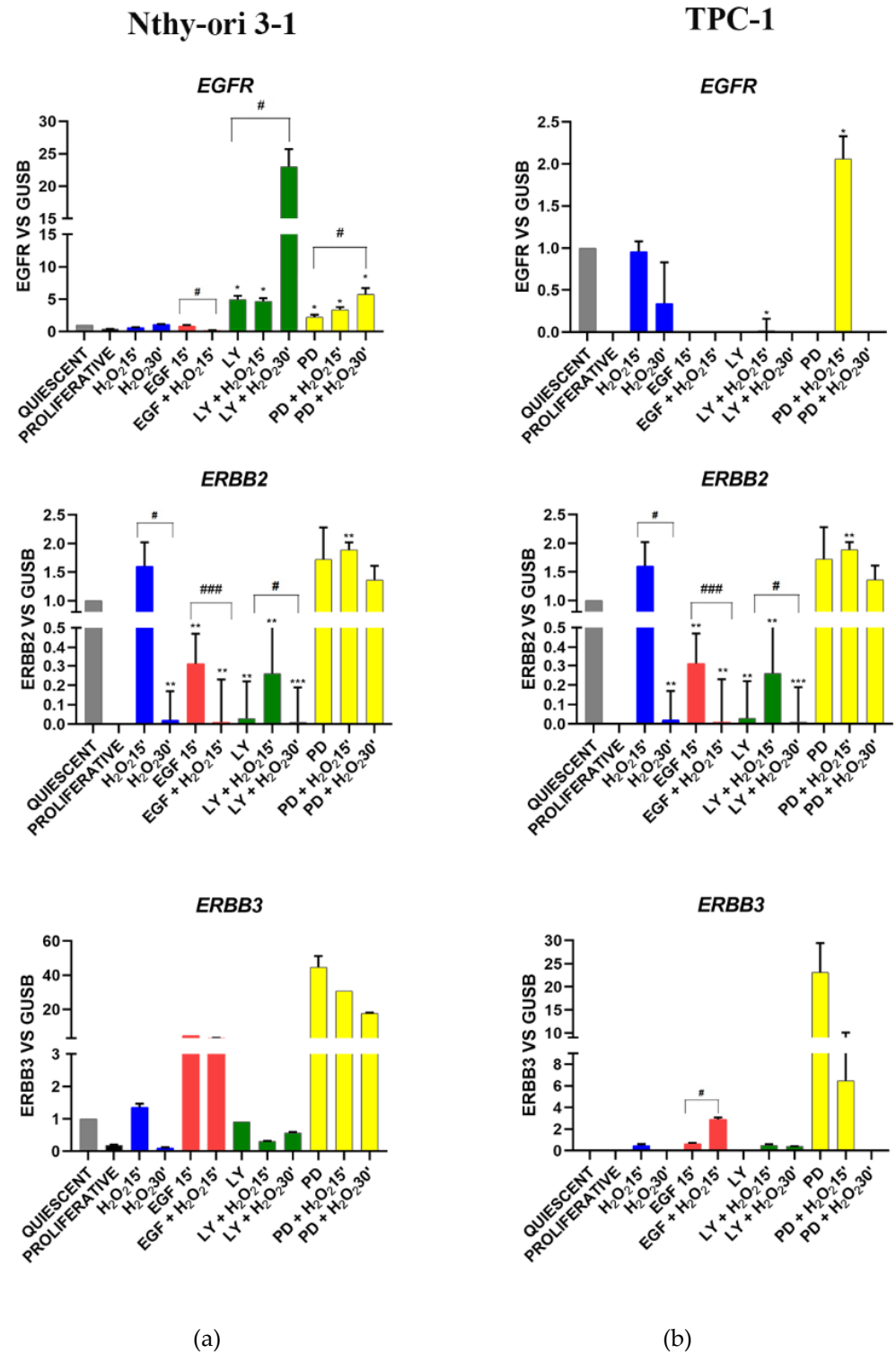


**Figure 4.** *EGFR* (epidermal growth factor receptor, *ERBB2* (Erb-B2 receptor tyrosine kinase 2), *ERBB3* (Erb-B3 receptor tyrosine kinase 3) gene expression modulation under H<sub>2</sub>O<sub>2</sub>, EGF, LY and PD treatments alone and combined in Nthy-ori 3-1 cells (a) vs. TPC-1 cells (b). Gene expression was analyzed by Real-time qPCR. The histogram represented normalized data with *GUSB* gene, and the results showed the average of three independent experiments. LY—LY294002; PD—PD98059; \*—*p* < 0.05, \*\*—*p* < 0.01 \*\*\*—*p* < 0.001 treated vs. quiescent cells; #—*p* < 0.05, ###—*p* < 0.001 cells with similar treatment.

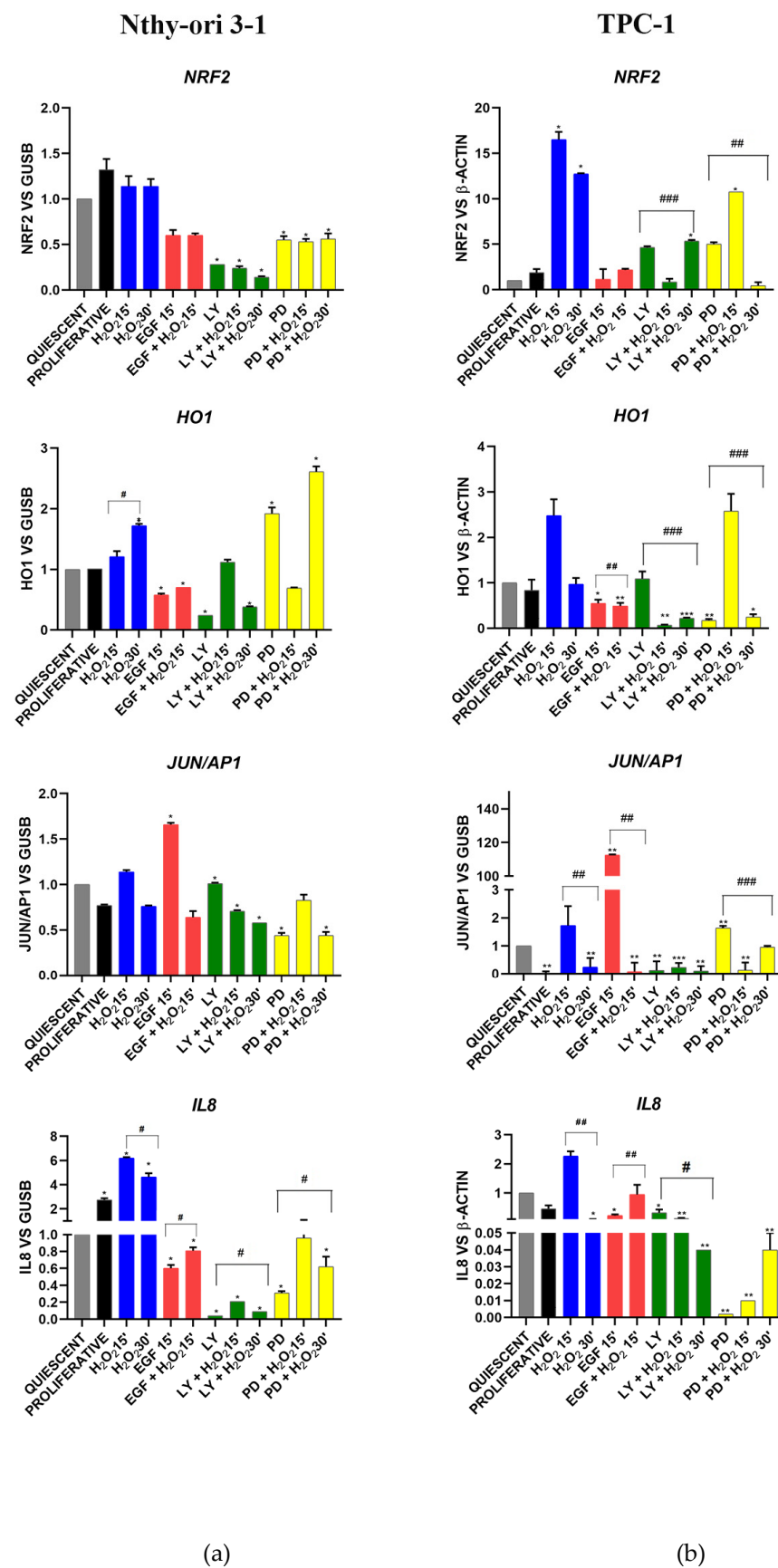


**Figure 5.** NRF2 (nuclear factor erythroid 2–related factor 2), HO1 (heme oxygenase 1), JUN/AP1 (Jun proto-oncogene, AP-1 transcription factor subunit) gene expression and IL8 (CXCL8, interleukin 8) modulation under H<sub>2</sub>O<sub>2</sub>, EGF, LY and PD treatments alone and combined in Nthy-ori 3-1 cells (a) vs.

TPC-1 cells (b). Gene expression was analyzed by real-time qPCR. The histogram represented normalized data with *GUSB* gene in Nthy-ori 3-1, while *NRF2* and *HO1* expression data were normalized with  $\beta$ -Actin in TPC-1 cells. The results showed the average of three independent experiments. LY—LY294002; PD—PD98059; \*— $p < 0.05$ ; \*\*— $p < 0.01$ ; \*\*\*— $p < 0.001$  treated vs. quiescent cells; #— $p < 0.05$ , ##— $p < 0.01$ , ###— $p < 0.001$  cells with similar treatment.

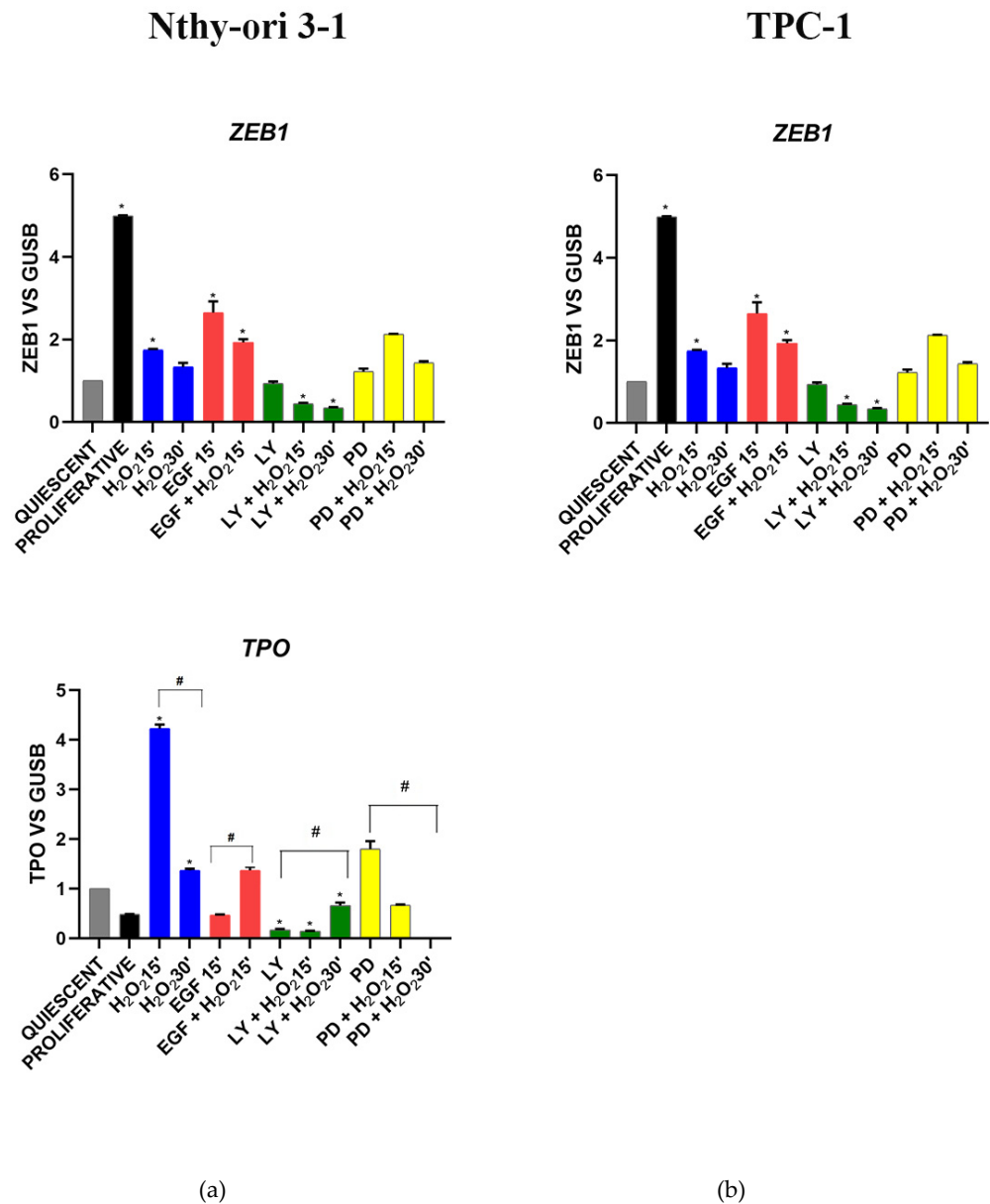


**Figure 6.** Gene expression modulation of *TPO* (thyroid peroxidase) and *ZEB-1* (zinc finger E-box binding homeobox 1) under H<sub>2</sub>O<sub>2</sub>, EGF, LY and PD treatments alone and combined. (a) Nthy-ori 3-1 cells, (b) TPC-1 cells. Gene expression was analyzed by real-time qPCR. The histogram represented normalized data with *GUSB* gene, and the results showed the average of three independent experiments. The expression of *TPO* was undetected in TPC-1 cells. LY—LY294002; PD—PD98059; \*— $p < 0.05$  treated vs. quiescent cells; #— $p < 0.05$  cells with similar treatment.

### 3.4. Gene Dosage Assay of *OGG1* and *MUTYH* in TPC1 Cells

Since TPC-1 cells did not express *MUTYH*, we evaluated the amount of genomic DNA (gDNA) of this gene and its partner *OGG1*. The qPCR data were normalized by the ratio on the value of endogenous *B-Actin* gDNA. The reference amount of the both alleles presence was validated on gDNA from Nthy-ori 3-1 cells; since the normalized values of

the controls (cell lines) matched perfectly, we were confident to employ this method to assay the TPC-1 cell line genome. In the TPC-1 cells, *OGG1* and *MUTYH* gDNA values did not show reduction (Figure 7).

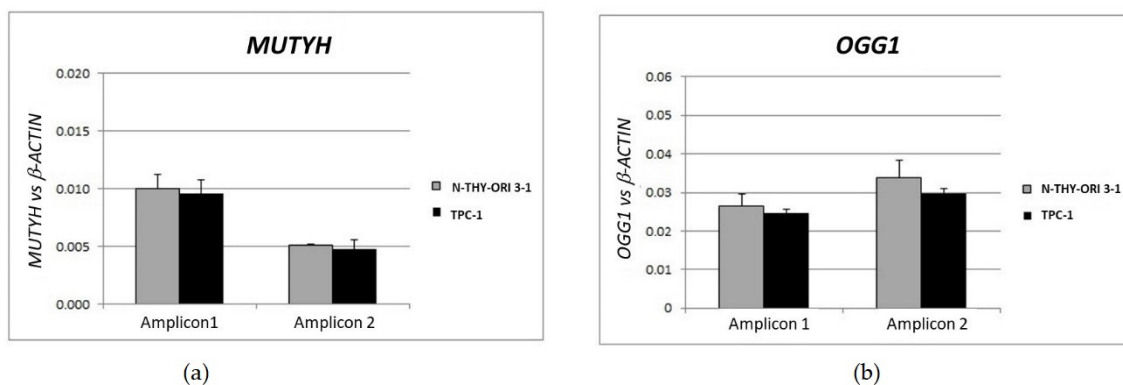


**Figure 7.** *MUTYH* and *OGG1* gene dosage. (a) Nthy-ori 3-1 cells, (b) TPC-1 cells. Gene dosage was performed by SYBR Green qRT-PCR. For both genes were selected two different genomic sequences. The samples were amplified in triplicate in three independent experiments. The gDNA amounts of the target genes were normalized by the ratio on median value of the *b-Actin* genomic reference gene from TPC-1 vs. Nthy-ori 3-1.

### 3.5. Gene Expression Cluster Analysis in Nthy-ori 3-1

To elucidate the potential cross-regulation between BER and EGFR pathways, we compared the genes expression levels detected in Nthy-ori 3-1 cells in response to the several treatments employing Multiexperiment viewer v4.0 program (MeV4.0) [35] (Figure 8). Under acute oxidative stress conditions (by 10 mM  $H_2O_2$  treatment), a close correlation among genes involved in stress response, i.e., *MUTYH*, *HO1* and *OGG1*, was observed. We also highlighted the correlation among *TPO*, *IL-8* and *JUN/AP1* transcription factor (Figure 8a).

When the Nthy-ori 3-1 cell line was stimulated by EGF, a strong relationship among the BER genes, *OGG1* and *APE1/Ref1* (alternatively named *APEX1*, *HAP1*, *APEN*), and antioxidant response gene, *NRF2* and *OH1* was shown; whereas *MUTYH* and *PPAR $\gamma$*  showed a correlation with *ErbB2* (Figure 8b). The inhibition of AKT pathway by LY, highlighted a lack of BER gene correlation, in addition to *APE1/Ref1*, was related to *NRF2*, *HO1* *IL-8* and *ErbB2* (Figure 8c). Interestingly, in normal thyroid cells the inhibition of MAPK (by PD) was the unique experimental condition that showed a correlation among the ErbB receptors (Figure 8d).

### 3.6. Protein Expression of ErbB Pathway and *OGG1* in Nthy-ori 3-1 and TPC-1 Cells

The effect induced by acute  $H_2O_2$  stress on ErbB and *OGG1* pathways was also assessed on protein expression. Western blotting analyses showed that the *OGG1* protein was expressed in quiescent Nthy-ori 3-1 cells, with clearly visible bands, at approximately 50 kDa (Figure 9a) [37,38]. This *OGG1* isoform was reduced or absent after  $H_2O_2$  treatments alone or combined with AKT and MAPK inhibitors (LY and PD, respectively). Instead, the same bands increased after PD and EGF treatment (Figure 9a), while EGF and  $H_2O_2$  co-treatment seemed to induce further *OGG1* post-transcriptional modifications, thus allowing the detection of 37kD isoform (Figure 9a).

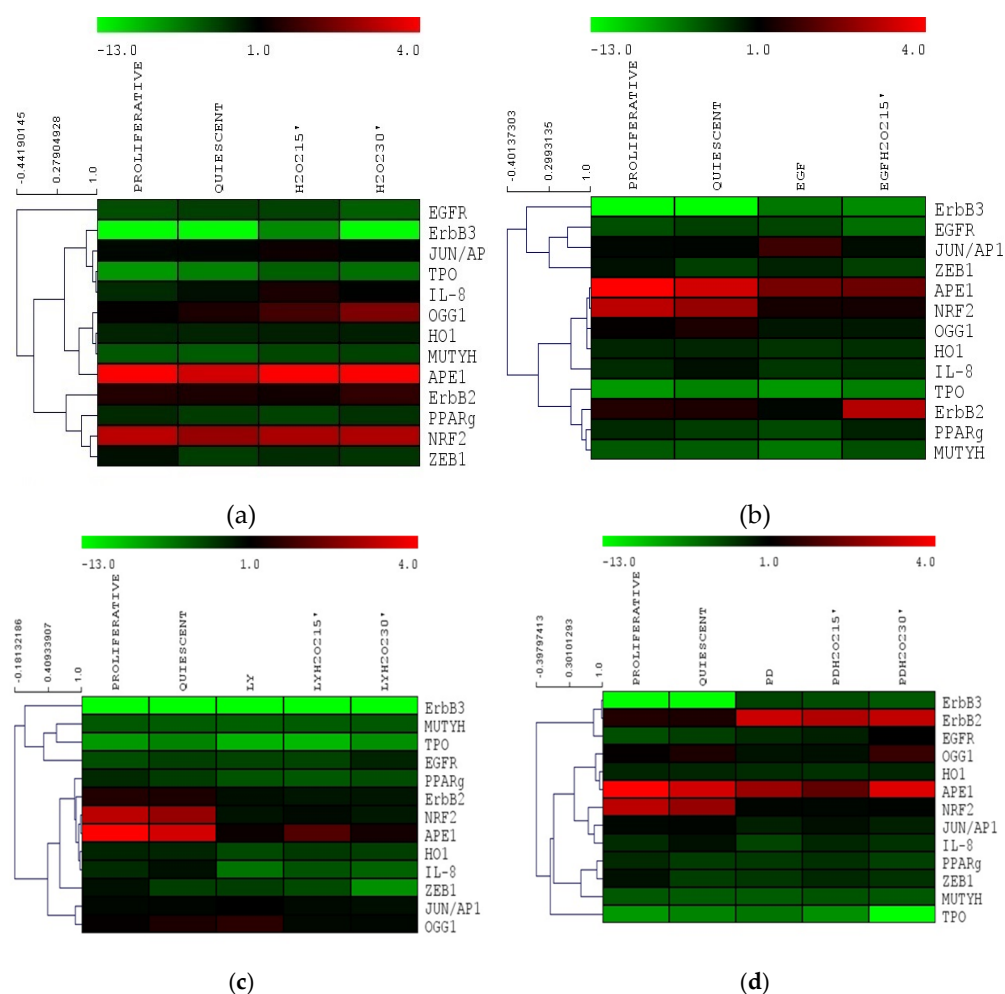


**Figure 8.** Gene expression cluster analysis by MeV4.9.0 in Nthy-ori 3-1 cells: (a)  $H_2O_2$  treatments; (b) EGF treatments; (c) LY treatments; (d) PD treatments. The average linkage hierarchical clustering with Pearson correlation was used. The color scale at the top represents the  $\log_2$  of every single gene expression value compared with housekeeping value ranging from  $-13$  (green) to  $4$  (red). The trees presented here are the neighbor-joining trees based on gene expression variation in response to different treatments. LY—LY294002; PD—PD98059.

The 37 kDa band, which should correspond to the nuclear OGG1 isoform (1a) [37] was increased by EGF and  $H_2O_2$  co-treatment. The level of PARP-1 protein expression was very mild in quiescent NThy-ori 3-1 and TPC-1 cells and the oxidative stress did not seem to modulate it (data not shown). Under all the experimental conditions we used, this protein resulted not cleaved, indicating that apoptosis (PARP-1-dependent) has not been activated.

Unlike what observed in normal Nthy-ori 3-1, in TPC-1 cells  $H_2O_2$  increased OGG1 expression after MAPK pathway inhibition, and EGF stimulation caused relevant changes respect to untreated quiescent cells (Figure 9a vs. Figure 9b). In Nthy-ori 3-1 cell line, the protein level of EGFR remained unchanged upon all treatments (data not shown), while, as expected, its phosphorylation in Tyr1068 was absent in starved untraded cells and appeared after EGF stimulation (Figure 9a). The acute stress by  $H_2O_2$  always induced EGFR phosphorylation even after inhibition of the AKT and MAPK. In all experimental conditions, ErbB2 was expressed and slightly reduced following oxidative stress (Figure 9a). In quiescent cells, MAPK phosphorylation was observed, while it was lightly inhibited by treatment with LY alone and with EGF plus  $H_2O_2$ . PD and  $H_2O_2$  co-treatment increased MAPK phosphorylation compared with PD alone. In quiescent untreated cells, a high level of phospho-AKT was detected, and  $H_2O_2$  treatment, after 30', inhibited it so as to

be undetected. PD treatment led a decrease in AKT phosphorylation which was more pronounced after co-treatment with H<sub>2</sub>O<sub>2</sub>.

Papillary thyroid cancer model TPC-1 did not express p-EGFR under any of the tested conditions (data not shown), whereas ErbB2 protein was always expressed and particularly increased after PD and EGF alone treatments (Figure 9b). The MAPK were activated in all experimental conditions especially with LY and H<sub>2</sub>O<sub>2</sub> co-treatment, contrary to what observed in normal cells. AKT was activated in the presence of H<sub>2</sub>O<sub>2</sub> also with PD and EGF alone. Relative expression quantification of the analyzed proteins in Nthy-ori3-1 and TPC-1 cells are visible in Figure 10.

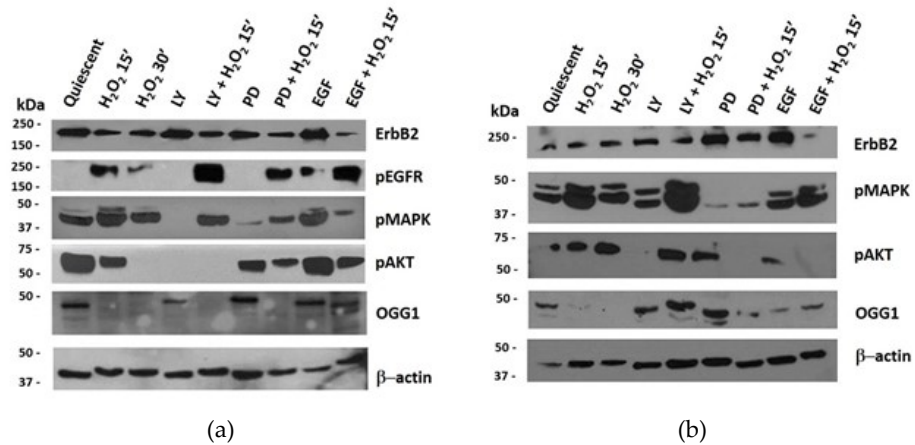


**Figure 9.** Protein expression and quantification in Nthy-ori 3-1 vs. TPC-1 cells. Nthy-ori 3-1 and TPC-1 cells were starved overnight and treated with, LY294002 (25 μM), PD98059 (50μM), EGF (50 ng/mL) alone and combined with H<sub>2</sub>O<sub>2</sub> (10 mM). Western blotting analysis in Nthy-ori 3-1 cells (a) and in TPC-1 cells (b) determining the protein expression levels of p-EGFR, ErbB2, p-MAPK, p-AKT and OGG1. Results are representative of three independent experiments. Quiescent cells were treated with H<sub>2</sub>O<sub>2</sub> and LY, PD, EGF alone or combined. LY—LY294002; PD—PD98059; kDa—protein molecular weight marker.

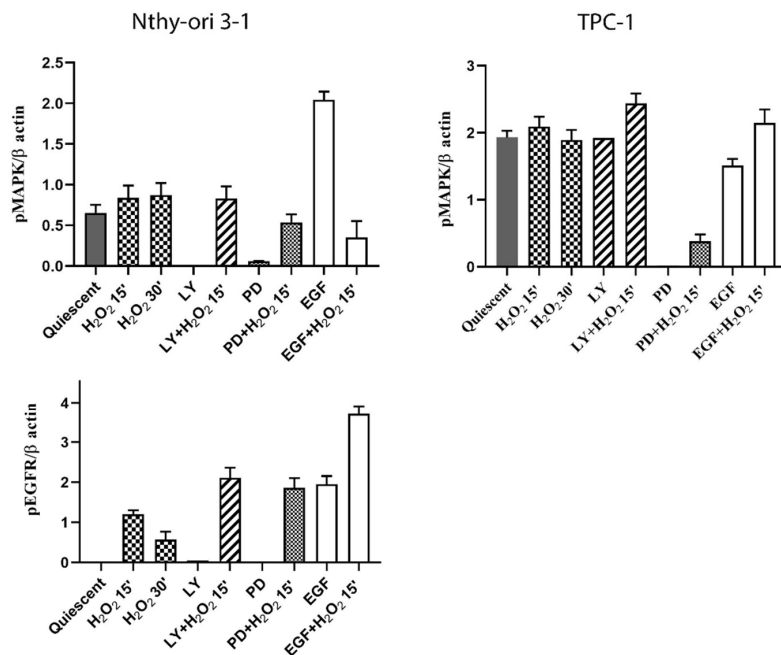


**Figure 10.** Cont.

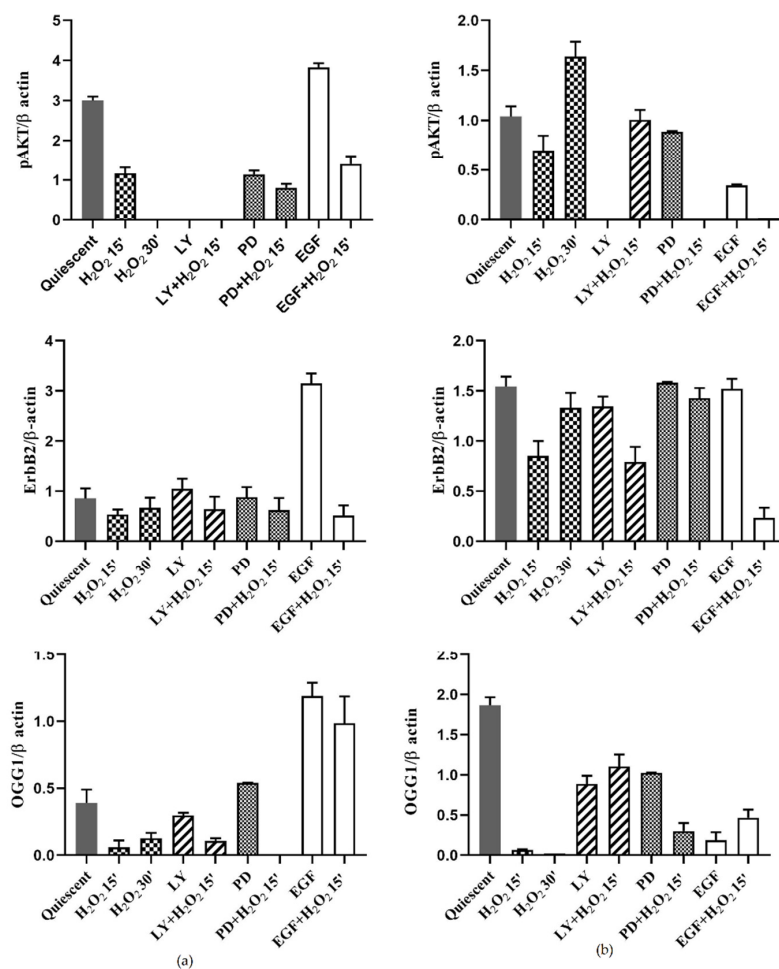


**Figure 10.** Protein expression quantification of ErbB pathway NThy-ori 3-1 vs. TPC-1 cells. Quantification of selected proteins (p-EGFR, ErbB2, p-MAPK, p-AKT) detected by WB in Nthy-ori3-1 and TPC-1 (Figure 9a,b). The expression of p-EGFR, was undetected in TPC-1 cells. The average expression levels of panel (a) and panel (b) were determined by densitometric analysis and calculated in relation to the  $\beta$ -Actin level. Quiescent cells were treated with  $H_2O_2$  and LY, PD, EGF alone or combined. LY—LY294002; PD—PD98059.

#### 4. Discussion

Thyroid diseases have a complex and multifactorial etiology [39]. Despite the numerous studies on the signals referable to the malignant transition [3], the molecular mechanisms concerning the role of oxidative stress in diseases and carcinogenesis of thyroid remain elusive. Indeed, it has long been believed that oxidative stress plays an active role in carcinogenesis and cancer progression [5]. One of the molecules with pro-oxidant characteristics is  $H_2O_2$ . It is physiologically produced and is involved in the adaptation to stress and in chronic inflammatory responses [9,10], but it is also actively produced in the thyroid as necessary for thyroid hormone synthesis. However, there are still many gaps in our knowledge regarding the cellular signaling network attributable to  $H_2O_2$  and to DNA damage in thyroid. Based on its strong oxidative power,  $H_2O_2$  in cancer cells with high proliferative rate could be responsible for the high level of oxidative DNA damage as observed in cancerous thyroid tissue [15] and hyperactivation of some signaling pathways [10] including mitogen-activated protein kinase (MAPK), and PI3K/Akt, involved in ErbB signaling [13,40].

Several studies on exposure of thyroid cells to irradiation or to nonlethal concentrations of  $H_2O_2$  have shown that  $H_2O_2$  can cause DNA damage, also supporting the hypothesis that  $H_2O_2$  generation in the thyroid could play a role in mutagenesis, especially when

antioxidant defense is deficient. [4]. Indeed, marked increases in the presence of 8-oxoG in nuclear and mitochondrial DNA were evident after treatment with H<sub>2</sub>O<sub>2</sub> or ionizing radiation. [16]. In aqueous solutions, as in the cellular interior, the reaction of H<sub>2</sub>O<sub>2</sub> with guanine leads to the formation of 8-oxoG complexed with a water molecule can occur according to two different mechanisms that have two steps each. The processes are described in detail by Jena et colleagues [41]. H<sub>2</sub>O<sub>2</sub> exposure has also been widely used to study the dynamics of 8-oxoG in mitochondrial DNA in wild-type and OGG1-deficient cell models. [42] Wang and colleagues used H<sub>2</sub>O<sub>2</sub> to simulate oxidative stress. They stated that although it is not a free radical, H<sub>2</sub>O<sub>2</sub> can circulate in cells and be efficiently converted to a hydroxyl radical and lead to an overall increase in genomic 8-oxoG level even in cells with wild-type OGG1. This increase in DNA lesions in proliferant cells was detected starting at 5 min of treatment, peaking at 15 min, and were then rapidly repaired by wild-type OGG1, restoring the redox balance. The authors also argued that the high level of 8-oxoG itself might not increase cell death [22].

In this study, we investigated the relationship between the EGFR and OGG1-BER pathways and its regulation following acute oxidative stress by H<sub>2</sub>O<sub>2</sub> in quiescent human thyroid cells. We evaluated, in both starved cell models, the effects of H<sub>2</sub>O<sub>2</sub> on cell viability. Initially, the range of concentrations chosen was supposed to mimic momentary distress compared with physiological amounts of H<sub>2</sub>O<sub>2</sub> produced by thyroid models in vitro [33], but also to what might be produced in the tissue microenvironment, e.g., under infectious and/or inflammatory conditions [10].

The H<sub>2</sub>O<sub>2</sub> response of cultured cells appears to depend on many factors [41]. In starved cells, we observed a rapid decline in cell viability after H<sub>2</sub>O<sub>2</sub> treatment due to H<sub>2</sub>O<sub>2</sub> interference with mitochondrial activity (Figure 1) and apoptosis/death (Figure S1) [43]. In additional analysis of cell cycle, after H<sub>2</sub>O<sub>2</sub> treatment, we did not observe sub-G1 cells in the H<sub>2</sub>O<sub>2</sub>-treated samples (Figure 2a). TPC-1 tumor cells showed a recovery of viability at 3 h with the lowest concentrations of H<sub>2</sub>O<sub>2</sub>, this phenomenon also appears to occur in other tumor cell models [44] and could be due to the multiple functional ormetic properties of H<sub>2</sub>O<sub>2</sub> in the cell context [44–46]. On the other hand, we must also consider that in thyrocytes the TPO downregulation, reducing its H<sub>2</sub>O<sub>2</sub> chemo-protective function, is involved in the evolution of nodularity towards the condition of tumorigenesis [47], in TPC-1 the expression of TPO was not detected. H<sub>2</sub>O<sub>2</sub> is a crucial substrate for thyroid peroxidase (TPO), a key enzyme involved in thyroid hormone synthesis [8]. On the plasma membrane of thyrocytes, TPO is associated with oxidoreductase dual oxidase 2 (DUOX2) and this functional interaction is essential for the regulation of the extracellular H<sub>2</sub>O<sub>2</sub> level [8].

Based on the above considerations, in this study we highlighted the crosstalk effect between EGFR and OGG1-BER on gene expression modulation, by stimulating starved thyroid cells with H<sub>2</sub>O<sub>2</sub> and EGF, and inhibiting EGFR its downstream ways, AKT and MAPK, using LY and PD (respectively) for a short time (15' and 30'). We assessed the physiological relationships between the two pathways using a normal thyroid cell line (Nthy-ori 3-1), and verified the dysregulations of these signals in TPC-1 tumor cells. Nthy-ori 3-1 cells were treated with H<sub>2</sub>O<sub>2</sub>, EGF, LY and PD alone and in combination. We observed that expression of genes involved in BER pathway, i.e., *OGG1*, *MUTYH*, *APE-1/Ref1* and *PPARγ*, exhibited generally the same trend, resulting upregulated by H<sub>2</sub>O<sub>2</sub> and downregulated by LY and PD. The *NRF2* gene expression decreased with EGF, LY and PD (with and without H<sub>2</sub>O<sub>2</sub>), while in contrast *OGG1* increased. This suggested that in thyroid *OGG1* may be regulated by a NRF2-independent way, in spite of the presence of an ARE (antioxidant response elements) region recognized by NRF2 in *OGG1* promoter [48]. In addition, the expression of the *HO1* gene, which responds both to oxidative stress and to NRF2-mediated gene regulation in different tissues [49], displayed a different behavior with respect to *NRF2*. These data did not completely exclude a role of NRF2 transcription factor in the response to acute oxidative stress in our system, because it is well-known that there are inactive form resides as subcellular compartmentalization pool bounded to Keap1 [50]. Gene expression cluster analysis showed that when Nthy-ori 3-1 cells were

stimulated with EGF and H<sub>2</sub>O<sub>2</sub>, *OGG1* and *APE1/Ref1* showed a strong correlation with *NRF2* and its downstream *HO1* and *IL8*. Instead, *MUTYH* demonstrated a correlation with *ErbB2* and *PPAR $\gamma$*  (Figure 8a,b). After LY treatment no significant correlation between any of the BER genes was shown (Figure 8c). Interestingly, MAPK inhibition (with PD) was the only experimental condition in which we observed a correlation between ErbB genes, this suggests a positive feedback mechanism in control gene expression (Figure 8d). Our results highlighted that the inhibition of ErbB receptors downstream pathways may have a role in dysregulation of the BER genes.

After inhibition of the AKT pathway, a correlation was observed between *OGG1* and *JUN/AP1* while after MAPK inhibition (Figure 8c,d), they correlated with CXC chemokine *IL-8* (also *CXCL8*) and *JUN/AP1*, as reported in the literature [51]. Therefore, the JUN/AP1 transcriptional activator could play a pivotal role in the correlation between the ErbB and BER systems (Figure 7).

Pro-inflammatory CXC chemokine *IL-8* (*CXCL8*) gene expression was significantly increased in Nthy-ori 3-1 proliferating cells and after H<sub>2</sub>O<sub>2</sub> treatments compared with starved cells. On the contrary, *IL-8* was reduced after EGF, LY and PD treatments alone and combined with H<sub>2</sub>O<sub>2</sub> (Figure 4). Our data confirmed that *IL-8* plays a role in response to oxidative stress that also stimulate its own production [52]. Interestingly, its synthesis may be dependent by EGFR activation [53]. *IL-8* was the first demonstrated chemokine to be secreted by human normal thyrocytes [54]. Moreover, the secretion of *IL-8* by cancer cells can enhance the proliferation and survival capabilities through an autocrine loop [53]. *MUTYH* gene in Nthy-ori 3-1 cells was clustered with other BER genes under oxidative stress conditions, whereas EGF induced a correlation with *PPAR $\gamma$*  and *ErbB2* (Figures 2 and 3), but this correlation was lost after LY and PD treatment suggesting that *MUTYH* gene expression might be regulated by EGFR pathways. Furthermore, gene expression data underlined a close correlation among *MUTYH*, *HO1* and *OGG1*, following H<sub>2</sub>O<sub>2</sub> treatment. In contrast, following EGF treatment, a close correlation among *MUTYH*, *PPAR $\gamma$*  and *ErbB2* was shown. These results confirmed the relationship between ErbB2 and *PPAR $\gamma$*  in regulating cell proliferation and metabolism as already displayed in other tissues [55]. It also highlights a bivalent role for *MUTYH*, under acute oxidative stress condition *MUTYH* showed a correlation with the other BER genes, probably because the primary necessity of cells is to defend itself from the high level of oxidative stress, whereas after EGF growth stimulus *MUTYH* showed a correlation with ErbB2 and *PPAR $\gamma$*  likely due to an increase in the metabolism rather than DNA repair, which becomes a secondary mechanism.

In Nthy-ori 3-1 cells, EGF treatment increased *ErbB2* gene expression only in combination with H<sub>2</sub>O<sub>2</sub>. The same effect was observed by blocking MAPK pathway by PD (Figure 3a). Under the effect of LY and PD, cotreated with H<sub>2</sub>O<sub>2</sub>, EGFR expression increased significantly (Figure 3a). These data were confirmed by protein analysis showing changes in EGFR receptor activation after H<sub>2</sub>O<sub>2</sub> treatment without altering its expression (Figure 9). These results led us to suggest the presence of fine-tuned mechanisms that regulate signals downstream of EGF and crosstalk with activities controlled by *OGG1* protein. The simultaneous presence of a factor that stimulates cellular growth (i.e., EGF) and adaptation to the H<sub>2</sub>O<sub>2</sub>-mediated oxidative stress, induced the expression of different isoforms of the *OGG1* in these cells. Our results showed that *OGG1* protein in normal thyroid cells was expressed in several isoforms depending on the treatments used (Figure 8). These findings could be explained both on the basis of that is currently known about this enzyme; an alternative splicing mechanism that acts on the C-terminal region was delineated. As a consequence, all isoforms share the N-terminal region but differ in C-terminal, determining the existence of several isoforms, such as the alternative splicing process of the C-terminal region of *OGG1* [35,36] and on post-translational modifications occurred as a response to the stress [56]. Currently, most of the activities of these isoforms are unknown.

In the normal system, *OGG1* was shown to be controlled by the AKT pathway as it also decreased in protein level, while the stimulation with EGF increased its expression in

many of its isoforms (Figure 9). Our results highlighted that the inhibition of ErbB receptors downstream pathways may have a role in modulation of the OGG1 end BER. This aspect is very dysregulated in the TPC-1 tumor cell which shows a strong expression of OGG1 despite the inhibition of AKT (Figure 9b).

In Nthy-ori cells, upon H<sub>2</sub>O<sub>2</sub> treatment, AKT activity decreased under all conditions tested, whereas in TPC-1 cells, AKT activity increased upon H<sub>2</sub>O<sub>2</sub> treatment. This difference in signaling between the two models could be explained by H<sub>2</sub>O<sub>2</sub>-driven deregulation in the mTOR pathways in TPC tumor model. H<sub>2</sub>O<sub>2</sub>, acting as an intracellular messenger, can activate phosphatidylinositol-3-kinase (PI3K) and its downstream target Akt, promoting cell survival. Accumulation of ROS has been associated with activation/phosphorylation of AKT to inactivation/phosphorylation of tuberin and activation of mTOR/complex II. Activation of adenosine-monophosphate-activated protein kinase (AMPK) by rapamycin may directly impact OGG1 activation or indirectly through blocking mTOR activity. This unusual activation of AKT is also followed by a higher protein level of OGG1 in the LY + H<sub>2</sub>O<sub>2</sub> condition, which is not reflected in mRNA levels. The increase in OGG1 was detected in several tumor cells treated to suppress mTOR activity. Rapamycin treatments can inhibit mTORC1 through increased phosphorylation of AMPK and lead to increased OGG1 activity. Although lower concentrations of rapamycin appeared to inhibit the activation of mTOR activation in cancer cells, higher concentrations were required to increase the protein and promoter activity of OGG1, suggesting that high concentrations of rapamycin may be required to activate other kinases, such as AMPK, in addition to blocking mTOR activity [57]. In support of this hypothesis, rapamycin increases the phosphorylation of AMPK, a signaling intermediate upstream of the mTOR pathway in several tumor cells. Activation of AMPK by rapamycin results in the inhibition of mTOR activity and increased protein expression and promoter activity of OGG1. In addition, activation of AMPK, by 5-aminoimidazole-4-carboxamide riboside (AICAR), resulted in inhibition of mTOR activity and increased promoter activity and protein expression of OGG1 in tuberin-deficient and von Hippel–Lindau (VHL) deficient cells [57].

The mechanism of regulation of cellular OGG1 protein, particularly in response to oxidative stress, is unclear. The stability of OGG1 is increased in response to oxidative stress induced by ionizing radiation. As a consequence of prolonged OGG1 stability and increased excision activity in the absence of E3 ubiquitin-protein ligase NEDD4-like, cells show increased DNA repair capacity but, conversely, this decreases post-irradiation cell survival. This effect may be reproduced upon overexpression of OGG1, suggesting that dysregulation of OGG1 increases intermediate DNA lesion formation [58]. Therefore, it would be very interesting to further investigate these functional aspects of OGG1 in papillary thyroid carcinoma with RET/TPC rearrangements.

Although OGG1-BER protects the genome integrity by repairing the lesion or eliminating cells with malignant potential and its overexpression improves H<sub>2</sub>O<sub>2</sub>-induced cell death [22], in the case of TPC-1 cells, the lack of *MUTYH* gene expression could favor the maintenance of tumor phenotype loop [59]. Furthermore, this confirms that OGG1, as a sensor in the BER response, can be controlled both at the gene and protein level by the Pi3K/AKT pathway, while this was not detected following stimulation by EGF and H<sub>2</sub>O<sub>2</sub>. Probably in quiescent TPC-1 cells, the presence of the RET/PTC rearrangement keeps the growth pathways independent of EGF stimulation by not expressing p-EGFR, as it appears to be (albeit slightly) in TPC-1 proliferating cells [60]. Molecular studies have also shown that RET/PTC in human thyrocytes promotes the activation of inflammation-related genes expression, and this could contribute to the progression and locoregional metastases, characteristic of the PTC tumors [60,61]. Stimulation of the OGG1 isoforms could also be caused by this aspect. Indeed, some studies have shown that the 8-oxoguanin glycosylase-1 repair enzyme is also involved in inflammation regulation and diseases [62,63].

TPC-1 cells showed a strong deregulation of the BER, OGG1 and *MUTYH*, components (Figure 2) with a loss in the gene expression of *MUTYH* and an increased expression of *APE-1/Ref1*. This result could be due to the presence of the RET/PTC rearrangement in the

papillary tumor model; indeed, oncogenic potential of RET/PTC is related to intrinsic tyrosine kinase activity and repression of p53-dependent transactivation [64]. Moreover, some previous studies have shown that the gene expression of *MUTYH* is controlled by TP53 [65] and that TP53 can also modulate the transcriptional activity of APE-1/Ref1 [66]. At present, these interactions between tyrosine kinase activities and BER signaling modulations have not yet been adequately explored in thyroid carcinogenesis and deserve further study.

## 5. Conclusions

Our observations highlighted that human thyroid cells, under acute oxidative stress, activate a physiological cross-regulation between the ErbB and OGG1-BER pathways. This regulation, assessed in a normal thyroid epithelial cell model and in a differentiated papillary cancer model, appeared to be dependent on H<sub>2</sub>O<sub>2</sub>- and EGF-related oxidative signals. This was evidenced by the significant positive response of OGG1 protein to inhibition of MAPK and AKT signaling, as well as the complete inhibition of *MUTYH* gene expression and the very strong increase in *APE1* gene expression. Our data on OGG1 protein expression suggest that it was physiologically regulated in response to oxidative modulation of ErbB, and that these might be dysregulated in the signaling pathway involving AKT in the progression of thyroid malignancies with RET/PTC rearrangements. Overall, this study suggests further investigation of the pathophysiological interactions of OGG1-BER pathways to elucidate the mechanisms underlying the onset and development of thyroid diseases.

**Supplementary Materials:** The following are available online at <https://www.mdpi.com/article/10.3390/cells11050822/s1>, Table S1: Details of primers for each evaluated gene by qRT-PCR and gene dosage assay, Figure S1: FACS analysis for FITC-Annexin-V-based apoptosis detection.

**Author Contributions:** C.M. contributed to study design, gene expression, data curation and wrote the manuscript; M.C.D.M., L.S. and E.D. performed cell cultures and protein analyses; R.C., G.M. and R.M. critically reviewed the manuscript; G.M.A. designed and coordinated the study and drafted the manuscript; G.S. performed gene dosage assay; P.S. and P.L. FACS analysis and data curation. All authors contributed to data analysis, drafting or revising the article, gave final approval of the version to be published, and agree to be accountable for all aspects of the work. All authors have read and agreed to the published version of the manuscript.

**Funding:** This research was funded by the “G. d’Annunzio” University of Chieti-Pescara (Fondi di Ateneo per la Ricerca–F.A.R.) grants to G.M.A., G.M., R.C. and R.M.

**Institutional Review Board Statement:** Not applicable.

**Informed Consent Statement:** Not applicable.

**Data Availability Statement:** The datasets used and/or analyzed during the current study are available from the corresponding author upon reasonable request.

**Conflicts of Interest:** The authors declare that they have no competing interest.

## Abbreviations

AMPK	adenosine-monophosphate-activated protein kinase
AKT	protein kinase B
BER	base excision repair
DUOX2	dual oxidase 2
APE1/Ref1	apurinic/aprimidinic endodeoxyribonuclease-1
EGFR	epidermal growth factor receptor
ErbB2	Erb-B2 receptor tyrosine kinase 2
ErbB3	Erb-B3 receptor tyrosine kinase 3
ErbB4	Erb-B4 receptor tyrosine kinase 4
GUSB	glucuronidase Beta
HO1	heme oxygenase 1
IL8	CXCL8, interleukin 8
Jun/AP1	Jun proto-oncogene, AP-1 transcription factor subunit
LY	LY294002;
MAPK	mitogen-activated protein kinase
MUTYH	mutY DNA glycosylase
NRF2	related factor
OGG1	8-oxoguanine glycosylase-1
PPAR $\gamma$	peroxisome-proliferator-activated receptor gamma
PTC	papillary thyroid carcinoma
ROS	reactive oxygen species
TPO	thyroid peroxidase
ZEB-1	zinc finger E-box-binding homeobox 1
PD	PD98059

## References

- Lim, H.; Devesa, S.S.; Sosa, J.A.; Check, D.; Kitahara, C.M. Trends in Thyroid Cancer Incidence and Mortality in the United States, 1974-2013. *JAMA* **2017**, *317*, 1338–1348. [[CrossRef](#)] [[PubMed](#)]
- Johnson, N.A.; Tublin, M.E. Postoperative surveillance of differentiated thyroid carcinoma: Rationale, techniques, and controversies. *Radiology* **2008**, *249*, 429–444. [[CrossRef](#)]
- Arora, N.; Scognamiglio, T.; Zhu, B.; Fahey, T.J. Do benign thyroid nodules have malignant potential? An evidence-based review. *World J. Surg.* **2008**, *32*, 1237–1246. [[CrossRef](#)]
- Ameziane El Hassani, R.; Buffet, C.; Leboulleux, S.; Dupuy, C. Oxidative stress in thyroid carcinomas: Biological and clinical significance. *Endocr. Relat. Cancer* **2019**, *26*, R131–R143. [[CrossRef](#)]
- Moloney, J.N.; Cotter, T.G. ROS signaling in the biology of cancer. *Semin. Cell Dev. Biol.* **2018**, *80*, 50–64. [[CrossRef](#)] [[PubMed](#)]
- Ekkholm, R. Iodination of thyroglobulin: An intracellular or extracellular process? *Mol. Cell. Endocrinol.* **1981**, *24*, 141–163. [[CrossRef](#)]
- Howie, A.F.; Arthur, J.R.; Nicol, F.; Walker, S.W.; Beech, S.G.; Beckett, G.J. Identification of a 57-kilodalton selenoprotein in human thyrocytes as thioredoxin reductase and evidence that its expression is regulated through the calcium-phosphoinositol signaling pathway. *J. Clin. Endocrinol. Metab.* **1998**, *83*, 2052–2058.
- Carvalho, D.P.; Dupuy, C. Thyroid hormone biosynthesis and release. *Mol. Cell. Endocrinol.* **2017**, *458*, 6–15. [[CrossRef](#)]
- Sigurdson, A.J.; Hauptmann, M.; Alexander, B.H.; Doody, M.M.; Thomas, C.B.; Struewing, J.P.; Jones, I.M. DNA damage among thyroid cancer and multiple cancer cases, controls, and long-lived individuals. *Mutat. Res.* **2005**, *586*, 173–188. [[CrossRef](#)]
- Sies, H. Hydrogen peroxide as a central redox signaling molecule in physiological oxidative stress: Oxidative eustress. *Redox Biol.* **2017**, *11*, 613–619. [[CrossRef](#)]
- Kumari, S.; Badana, A.K.; Mohan, G.M.; Shailender, G.; Malla, R. Reactive Oxygen Species: A Key Constituent in Cancer Survival. *Biomark. Insights* **2018**, *13*, 1177271918755391. [[CrossRef](#)] [[PubMed](#)]
- Weng, M.S.; Chang, J.H.; Hung, W.Y.; Yang, Y.C.; Chien, M.H. The interplay of reactive oxygen species and the epidermal growth factor receptor in tumor progression and drug resistance. *J. Exp. Clin. Cancer Res.* **2018**, *37*, 61. [[CrossRef](#)] [[PubMed](#)]
- Metere, A.M.; Frezzotti, F.; Graves, C.E.; Vergine, M.; De Luca, A.; Pietraforte, D.; Giacomelli, L.A. Possible role for selenoprotein glutathione peroxidase (GPx1) and thioredoxin reductases (TrxR1) in thyroid cancer: Our experience in thyroid surgery. *Cancer Cell Int.* **2018**, *18*, 7. [[CrossRef](#)] [[PubMed](#)]
- Szanto, I.; Pusztaszeri, M.; Mavromati, M. H<sub>2</sub>O<sub>2</sub> Metabolism in Normal Thyroid Cells and in Thyroid Tumorigenesis: Focus on NADPH Oxidases. *Antioxidants* **2019**, *8*, 126. [[CrossRef](#)]

15. Yi, J.W.; Park, J.Y.; Sung, J.Y.; Kwak, S.H.; Yu, J.; Chang, J.H.; Kim, J.H.; Ha, S.Y.; Paik, E.K.; Lee, W.S.; et al. Genomic evidence of reactive oxygen species elevation in papillary thyroid carcinoma with Hashimoto thyroiditis. *Endocr. J.* **2015**, *62*, 857–877. [[CrossRef](#)]
16. Soutanakis, R.P.; Melamede, R.J.; Bespalov, I.A.; Wallace, S.S.; Beckman, K.B.; Ames, B.N.; Taatjes, D.J.; Janssen-Heininger, Y.M. Fluorescence detection of 8-oxoguanine in nuclear and mitochondrial DNA of cultured cells using a recombinant Fab and confocal scanning laser microscopy. *Free Radic. Biol. Med.* **2000**, *28*, 987–998. [[CrossRef](#)]
17. Mo, J.Y.; Maki, H.; Sekiguchi, M. Hydrolytic elimination of a mutagenic nucleotide, 8-oxodGTP by human 18-kilodalton protein: Sanitization of nucleotide pool. *Proc. Natl. Acad. Sci. USA* **1992**, *89*, 11021–11025. [[CrossRef](#)]
18. Oka, S.; Leon, J.; Tsuchimoto, D.; Sakumi, K.; Nakabeppu, Y. MUTYH, an adenine DNA glycosylase, mediates p53 tumor suppression via PARP-dependent cell death. *Oncogenesis*. **2015**, *4*, e142. [[CrossRef](#)]
19. Banda, D.M.; Nuñez, N.N.; Burnside, M.A.; Bradshaw, K.M.; David, S.S. Repair of 8-oxoG:A mismatches by the MUTYH glycosylase: Mechanism, metals and medicine. *Free Radic. Biol. Med.* **2017**, *107*, 202–215. [[CrossRef](#)]
20. Paschke, R. Molecular pathogenesis of nodular goiter. *Langenbecks Arch. Surg.* **2011**, *396*, 1127–1397. [[CrossRef](#)]
21. Sivilar, D.; Goellner, E.M.; Almeida, K.H.; Sobol, R.W. Base excision repair and lesion-dependent subpathways for repair of oxidative DNA damage. *Antioxid. Redox Signal* **2011**, *14*, 2491–2507. [[CrossRef](#)]
22. Wang, R.; Li, C.; Qiao, P.; Xue, Y.; Zheng, X.; Chen, H.; Zeng, X.; Liu, W.; Boldogh, I.; Ba, X. OGG1-initiated base excision repair exacerbates oxidative stress-induced parthanatos. *Cell Death Dis.* **2018**, *9*, 628. [[CrossRef](#)] [[PubMed](#)]
23. Mincione, G.; Di Marcantonio, M.C.; Tarantelli, C.; D’Inzeo, S.; Nicolussi, A.; Nardi, F.; Donini, C.F.; Coppa, A. EGF and TGF- $\beta$ 1 Effects on Thyroid Function. *J. Thyroid Res.* **2011**, *2011*, 431718. [[CrossRef](#)] [[PubMed](#)]
24. Ely, A.; Bischoff, L.A.; Weiss, V.L. Wnt signaling in thyroid homeostasis and carcinogenesis. *Genes* **2018**, *9*, 204. [[CrossRef](#)]
25. Chen, D.J.; Nirodi, C.S. The epidermal growth factor receptor: A role in repair of radiation-induced DNA damage. *Clin. Cancer Res.* **2007**, *13*, 6555–6560. [[CrossRef](#)]
26. Bensimon, A.; Aebersold, R.; Shiloh, Y. Beyond ATM: The protein kinase landscape of the DNA damage response. *FEBS Lett.* **2011**, *585*, 1625–1639. [[CrossRef](#)]
27. Oberthür, R.; Seemann, H.; Gehrig, J.; Rave-Fränk, M.; Bremmer, F.; Halpape, R.; Conradi, L.C.; Scharf, J.G.; Burfeind, P.; Kaulfuß, S. Simultaneous inhibition of IGF1R and EGFR enhances the efficacy of standard treatment for colorectal cancer by the impairment of DNA repair the induction of cell death. *Cancer. Lett.* **2017**, *407*, 93–105. [[CrossRef](#)]
28. Saiselet, M.; Floor, S.; Tarabichi, M.; Dom, G.; Hébrant, A.; van Staveren, W.C.; Maenhaut, C. Thyroid cancer cell lines: An overview. *Front. Endocrinol.* **2012**, *3*, 133. [[CrossRef](#)]
29. Nicolussi, A.; D’Inzeo, S.; Mincione, G.; Buffone, A.; Di Marcantonio, M.C.; Cotellesse, R.; Cichella, A.; Capalbo, C.; Di Gioia, C.; Nardi, F.; et al. PRDX1 and PRDX6 are repressed in papillary thyroid carcinomas via BRAF V600E-dependent and -independent mechanisms. *Int. J. Oncol.* **2014**, *44*, 548–556. [[CrossRef](#)] [[PubMed](#)]
30. Pirkmajer, S.; Chibalin, A.V. Serum starvation: Caveat emptor. *Am. J. Physiol. Cell. Physiol.* **2011**, *301*, C272–C279. [[CrossRef](#)]
31. Massart, C.; Hoste, C.; Virion, A.; Ruf, J.; Dumont, J.E.; Van Sande, J. Cell biology of H<sub>2</sub>O<sub>2</sub> generation in the thyroid: Investigation of the control of dual oxidases (DUOX) activity in intact ex vivo thyroid tissue and cell lines. *Mol. Cell Endocrinol.* **2011**, *343*, 32–44. [[CrossRef](#)]
32. Lanuti, P.; Fuhrmann, S.; Lachmann, R.; Marchisio, M.; Miscia, S.; Kern, F. Simultaneous characterization of phospho-proteins and cell cycle in activated T cell subsets. *Int. J. Immunopathol. Pharmacol.* **2009**, *22*, 689–698. [[CrossRef](#)] [[PubMed](#)]
33. Bologna, G.; Lanuti, P.; D’Ambrosio, P.; Tonucci, L.; Pierdomenico, L.; D’Emilio, C.; Celli, N.; Marchisio, M.; d’Alessandro, N.; Santavenere, E.; et al. Water-soluble platinum phthalocyanines as potential antitumor agents. *Biomaterials* **2014**, *27*, 575–589. [[CrossRef](#)]
34. Moscatello, C.; Di Nicola, M.; Veschi, S.; Di Gregorio, P.; Cianchetti, E.; Stuppia, L.; Battista, P.; Cama, A.; Curia, M.C.; Aceto, G.M. Relationship between MUTYH, OGG1 and BRCA1 mutations and mRNA expression in breast and ovarian cancer predisposition. *Mol. Clin. Oncol.* **2021**, *14*, 15. [[CrossRef](#)]
35. Aceto, G.M.; Fantini, F.; De Iure, S.; Di Nicola, M.; Palka, G.; Valanzano, R.; Di Gregorio, P.; Stigliano, V.; Genuardi, M.; Battista, P.; et al. Correlation between mutations and mRNA expression of APC and MUTYH genes: New insight into hereditary colorectal polyposis predisposition. *J. Exp. Clin. Cancer Res.* **2015**, *34*, 131. [[CrossRef](#)]
36. Saeed, A.I.; Sharov, V.; White, J.; Li, J.; Liang, W.; Bhagabati, N.; Braisted, J.; Klapa, M.; Currier, T.; Thiagarajan, M.; et al. TM4: A free, open-source system for microarray data management and analysis. *Biotechniques* **2003**, *34*, 374–378. [[CrossRef](#)] [[PubMed](#)]
37. Furihata, C. An active alternative splicing isoform of human mitochondrial 8-oxoguanine DNA glycosylase (OGG1). *Genes Environ.* **2015**, *37*, 21. [[CrossRef](#)] [[PubMed](#)]
38. Pal, R.; Ramdzan, Z.M.; Kaur, S.; Duquette, P.M.; Marcotte, R.; Leduy, L.; Davoudi, S.; Lamarche-Vane, N.; Iulianella, A.; Nepveu, A. CUX2 protein functions as an accessory factor in the repair of oxidative DNA damage. *J. Biol. Chem.* **2015**, *290*, 22520–22531. [[CrossRef](#)] [[PubMed](#)]
39. Böttcher, Y.; Eszlinger, M.; Tönjes, A.; Paschke, R. The genetics of euthyroid familial goiter. *Trends Endocrinol. Metab.* **2005**, *16*, 314–319. [[CrossRef](#)]
40. Yarden, Y.; Sliwkowski, M.X. Untangling the ErbB signaling network. *Nat. Rev. Mol. Cell Biol.* **2001**, *2*, 127–137. [[CrossRef](#)]
41. Jena, N.R.; Mishra, P.C. Mechanisms of formation of 8-oxoguanine due to reactions of one and two OH\* radicals and the H<sub>2</sub>O<sub>2</sub> molecule with guanine: A quantum computational study. *J. Phys. Chem. B* **2005**, *109*, 14205–14218. [[CrossRef](#)] [[PubMed](#)]

42. Ohno, M.; Oka, S.; Nakabeppu, Y. Quantitative analysis of oxidized guanine, 8-oxoguanine, in mitochondrial DNA by immunofluorescence method. *Methods Mol. Biol.* **2009**, *554*, 199–212. [[PubMed](#)]
43. Barbouti, A.; Amorgianiotis, C.; Kolettas, E.; Kanavaros, P.; Galaris, D. Hydrogen peroxide inhibits caspase-dependent apoptosis by inactivating procaspase-9 in an iron-dependent manner. *Free Radic. Biol. Med.* **2007**, *43*, 1377–1387. [[CrossRef](#)] [[PubMed](#)]
44. Halliwell, B. Cell culture, oxidative stress, and antioxidants: Avoiding pitfalls. *Biomed J.* **2014**, *37*, 99–105. [[CrossRef](#)]
45. Gorrini, C.; Harris, I.S.; Mak, T.W. Modulation of oxidative stress as an anticancer strategy. *Nat. Rev. Drug. Discov.* **2013**, *12*, 931–947. [[CrossRef](#)]
46. Wu, W.S. The signaling mechanism of ROS in tumor progression. *Cancer Metastasis Rev.* **2006**, *25*, 695–705. [[CrossRef](#)]
47. Knobel, M.; Medeiros-Neto, G. An outline of inherited disorders of the thyroid hormone generating system. *Thyroid* **2003**, *13*, 771–801. [[CrossRef](#)]
48. Kim, K.C.; Lee, I.K.; Kang, K.A.; Cha, J.W.; Cho, S.J.; Na, S.Y.; Chae, S.; Kim, H.S.; Kim, S.; Hyun, J.W. 7,8-Dihydroxyflavone suppresses oxidative stress-induced base modification in DNA via induction of the repair enzyme 8-oxoguanine DNA glycosylase-1. *BioMed Res. Int.* **2013**, *2013*, 863720. [[CrossRef](#)]
49. Loboda, A.; Damulewicz, M.; Pyza, E.; Jozkowicz, A.; Dulak, J. Role of Nrf2/HO-1 system in development, oxidative stress response and diseases: An evolutionarily conserved mechanism. *Cell Mol. Life Sci.* **2016**, *73*, 3221–3247. [[CrossRef](#)]
50. Wang, L.; Jiang, H.; Yin, Z.; Aschner, M.; Cai, J. Methylmercury toxicity and Nrf2-dependent detoxification in astrocytes. *Toxicol. Sci.* **2009**, *107*, 135–143. [[CrossRef](#)]
51. Natarajan, R.; Gupta, S.; Fisher, B.J.; Ghosh, S.; Fowler, A.A., 3rd. Nitric oxide suppresses IL-8 transcription by inhibiting c-Jun N-terminal kinase-induced AP-1 activation. *Exp. Cell. Res.* **2001**, *266*, 203–212. [[CrossRef](#)] [[PubMed](#)]
52. Paszti-Gere, E.; Szeker, K.; Csibrik-Nemeth, E.; Csizinszky, R.; Marosi, A.; Palocz, O.; Farkas, O.; Galfi, P. Metabolites of *Lactobacillus plantarum* 2142 prevent oxidative stress-induced overexpression of proinflammatory cytokines in IPEC-J2 cell line. *Inflammation* **2012**, *35*, 1487–1499. [[CrossRef](#)] [[PubMed](#)]
53. Waugh, D.J.; Wilson, C. The interleukin-8 pathway in cancer. *Clin. Cancer Res.* **2008**, *14*, 6735–6741. [[CrossRef](#)]
54. Weetman, A.P.; Bennett, G.L.; Wong, W.L. Thyroid follicular cells produce interleukin-8. *J. Clin. Endocrinol. Metab.* **1992**, *75*, 328–330. [[PubMed](#)]
55. Menendez, J.A. Fine-tuning the lipogenic/lipolytic balance to optimize the metabolic requirements of cancer cell growth: Molecular mechanisms and therapeutic perspectives. *Biochim. Biophys. Acta.* **2010**, *1801*, 381–391. [[CrossRef](#)]
56. Carter, R.J.; Parsons, J.L. Base Excision Repair a Pathway Regulated by Posttranslational Modifications. *Mol. Cell. Biol.* **2016**, *36*, 1426–1437. [[CrossRef](#)] [[PubMed](#)]
57. Habib, S.L. Mechanism of activation of AMPK and upregulation of OGG1 by rapamycin in cancer cells. *Oncotarget* **2011**, *2*, 958–959. [[CrossRef](#)]
58. Hughes, J.R.; Parsons, J.L. The E3 Ubiquitin Ligase NEDD4L Targets OGG1 for Ubiquitylation and Modulates the Cellular DNA Damage Response. *Front Cell Dev. Biol.* **2020**, *12*, 607060. [[CrossRef](#)] [[PubMed](#)]
59. Curia, M.C.; Catalano, T.; Aceto, G.M. MUTYH: Not just polyposis. *World J. Clin. Oncol.* **2020**, *11*, 428–449. [[CrossRef](#)] [[PubMed](#)]
60. Frasca, F.; Vella, V.; Nicolosi, M.L.; Messina, R.L.; Gianì, F.; Lotta, S.; Vigneri, P.; Regalbuto, C.; Vigneri, R. Thyroid cancer cell resistance to gefitinib depends on the constitutive oncogenic activation of the ERK pathway. *J. Clin. Endocrinol. Metab.* **2013**, *98*, 2502–2512. [[CrossRef](#)]
61. Borrello, M.G.; Alberti, L.; Fischer, A.; Degl'innocenti, D.; Ferrario, C.; Gariboldi, M.; Marchesi, F.; Allavena, P.; Greco, A.; Collini, P.; et al. Induction of a proinflammatory program in normal human thyrocytes by the RET/PTC1 oncogene. *Proc. Natl. Acad. Sci. USA* **2005**, *102*, 14825–14830. [[CrossRef](#)] [[PubMed](#)]
62. Li, G.; Yuan, K.; Yan, C.; Fox, J., 3rd; Gaid, M.; Breitwieser, W.; Bansal, A.K.; Zeng, H.; Gao, H.; Wu, M. 8-Oxoguanine-DNA glycosylase 1 deficiency modifies allergic airway inflammation by regulating STAT6 and IL-4 in cells and in mice. *Free Radic Biol. Med.* **2012**, *52*, 392–401. [[CrossRef](#)] [[PubMed](#)]
63. Ba, X.; Aguilera-Aguirre, L.; Rashid, Q.T.; Bacsi, A.; Radak, Z.; Sur, S.; Hosoki, K.; Hegde, M.L.; Boldogh, I. The role of 8-oxoguanine DNA glycosylase-1 in inflammation. *Int. J. Mol. Sci.* **2014**, *15*, 16975–16997. [[CrossRef](#)] [[PubMed](#)]
64. Kim, D.W.; Hwang, J.H.; Suh, J.M.; Kim, H.; Song, J.H.; Hwang, E.S.; Hwang, I.Y.; Park, K.C.; Chung, H.K.; Kim, J.M.; et al. RET/PTC (rearranged in transformation/papillary thyroid carcinomas) tyrosine kinase phosphorylates and activates phosphoinositide-dependent kinase1 (PDK1): An alternative phosphatidylinositol 3-kinase-independent pathway to activate PDK1. *Mol. Endocrinol.* **2003**, *17*, 1382–1394. [[CrossRef](#)] [[PubMed](#)]
65. Oka, S.; Nakabeppu, Y. DNA glycosylase encoded by MUTYH functions as a molecular switch for programmed cell death under oxidative stress to suppress tumorigenesis. *Cancer Sci.* **2011**, *102*, 677–682. [[CrossRef](#)] [[PubMed](#)]
66. Uddin, M.A.; Akhter, M.S.; Siejka, A.; Catravas, J.D.; Barabutis, N. P53 supports endothelial barrier function via APE1/Ref1 suppression. *Immunobiology* **2019**, *224*, 532–538. [[CrossRef](#)]